Food Hydrocolloids 148 (2024) 109429

Contents lists available at ScienceDirect

Food Hydrocolloids

journal homepage: www.elsevier.com/locate/foodhyd

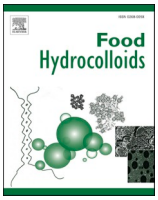

Pea protein globulins: Does their relative ratio matter?

Holly Husband, Sungil Ferreira, Fan Bu, Samira Feyzi, Baraem P. Ismail *

Food Science and Nutrition Department, University of Minnesota, 1334 Eckles Ave, Saint Paul, Minnesota, 55108, United States

ARTICLE INFO

Keywords:
Pea protein
7S vicilin/11S legumin ratio
Structural characteristics
Functional properties
Nutritional quality

ABSTRACT

The relatively low abundance of 11S legumin in pea protein, coupled with the wide diversity in 7S vicilin to 11S legumin ratio among pea protein ingredients, are assumed contributors to inferior and inconsistent properties relative to soy protein. To improve the performance of pea protein ingredients in food applications, optimum protein profile must be identified. Therefore, this work followed a holistic approach to determine the impact of 7S/11S ratio on pea protein structure, functionality, and nutritional quality. Vicilin- and legumin-rich fractions were isolated and combined in different proportions to produce samples of varying 7S/11S ratios. For the first time, pea protein isolate was also enriched with 11S legumin to evaluate the impact of 11S abundance on functionality within an unfractionated protein matrix. The low abundance of 11S in pea protein did not seem to be the cause of inferior properties. In fact, 7S vicilin had 6-fold higher gel strength and 5-fold higher emulsification capacity, but significantly lower nutritional quality, than 11S legumin. Despite having significantly higher sulfur-containing amino acids, high protein polymerization in 11S legumin contributed to relatively low functionality. Further, fractionation induced unique changes to amino acid composition, resulting in significantly lower amino acid scores for isolated 7S vicilin and 11S legumin relative to pea protein isolate. Accordingly, 11S legumin enrichment of pea protein isolate did not improve functionality or nutritional quality. Nevertheless, this work contributed foundational knowledge that will provide direction for future studies aiming at devising strategies to improve the quality and consistency of pea protein ingredients.

1. Introduction

In the United States, grocery sales of plant-based foods grew 54% in the last three years and have reached a market value of $7.4 billion (SPINS/GFI, 2021). Soy protein is the principal protein ingredient in many plant-based products across categories (McClements & Grossmann, 2022). The soy protein dominance in the plant protein market is attributed to many decades of research that led to a comprehensive understanding of its excellent functionality and nutritional quality (Uzzan, 1988; Waggle, Steinke, & Shen, 1989). However, pea protein is attracting interest as a soy protein replacement due to its current non-allergenic, non-GMO status. In fact, pea protein is one of the fastest growing plant proteins in global alternative product launches, with its rampant growth attributed to the agronomic benefits of growing pea, low production cost, and acceptable nutritional quality (Barac et al., 2010; Grand View Research, 2021). Furthermore, as legumes, pea and soy have a considerable homology in their protein components (Danielsson, 1949; Schroeder, 1982). The major protein components in pea, 7S vicilin and 11S legumin, have similar molecular weight, amino acid composition, and subunit structures to their counterparts in soy, 7S β-conglycinin and 11S glycinin (Derbyshire, Wright, & Boulter, 1976). The 7S and 11S proteins are largely responsible for protein functionality and nutritional quality in foods (Gueguen & Barbot, 1988; Tulbek, Lam, Wang, Asavajaru, & Lam, 2017).

Despite having similar profile, pea protein has inferior functionality in food and beverage applications compared to soy protein (Zhao, Shen, Wu, Zhang, & Xu, 2020). This inferiority may be in part explained by the differences in the 7S/11S ratio between pea and soy. The ratio of 7S/11S in soy may range from 0.47 to 0.79 across cultivars (Murphy & Resurreccion, 1984; Tzitzikas, Vincken, De Groot, Gruppen, & Visser, 2006). This regularity in protein profile among soy cultivars, coupled with the consistently larger abundance of the highly functional 11S glycinin over 7S β-conglycinin, have led to consistent functionality and nutritional quality of soy protein ingredients (Rutherfurd, Fanning, Miller, & Moughan, 2014; Tzitzikas et al., 2006). Meanwhile, a much wider diversity in the 7S/11S ratio in pea has been reported, ranging from 0.2 to

* Corresponding author. 1334 Eckles Avenue, St Paul, MN 55108, United States.
E-mail addresses: husba023@umn.edu (H. Husband), sungilferreira@gmail.com (S. Ferreira), bu007102@umn.edu (F. Bu), sfeyzi@umn.edu (S. Feyzi), bismailm@umn.edu (B.P. Ismail).

https://doi.org/10.1016/j.foodhyd.2023.109429
Received 13 April 2023; Received in revised form 26 September 2023; Accepted 15 October 2023
Available online 19 October 2023
0268-005X/

8.0 depending on factors such as agronomic practices, environmental conditions, and most importantly, genetic origin (Casey, Sharman, Wright, Bacon, & Guldager, 1982; Mertens, Dehon, Bourgeois, Verhaeghe-Cartrysse, & Blecker; 2012). These factors also cause differences in protein subunit composition and conformation, which contribute to heterogeneity beyond the 7S/11S ratio (Derbyshire et al., 1976). The culmination of these variances has significant implications on pea protein functionality and nutritional quality (Casey et al., 1982; Gueguen & Barbot, 1988). Barac et al. (2010) and O'KaneVereijken, Gruppen, and Van Boekel (2005) reported that pea proteins from different genotypes had significantly different emulsifying and gelling properties, respectively. In addition, the protein digestibility corrected amino acid score (PDCAAS) for pea protein fluctuated between 0.54 and 0.89 among different cultivars (Mertens, Dehon, Bourgeois, Verhaeghe-Cartrysse, & Blecker, 2012; Nosworthy & House, 2017; Rutherfurd et al., 2014).

In attempts to investigate the effects of pea protein variance on its functionality, researchers isolated 7S vicilin and/or 11S legumin from a specific pea cultivar, mixed them in varying ratios, and evaluated structural and functional properties. Dagorn-Scaviner, Gueguen, and Lefebvre (1986, 1987) mixed pea 7S vicilin and 11S legumin in four different 7S/11S ratios (0.33, 0.5, 1.0, and 3.0), and determined that vicilin had greater surface activity and emulsifying properties than legumin. In contrast, Koyoro and Powers (1987) found that purified legumin had higher emulsification capacity than purified vicilin and a 7S/11S mixture (unspecified ratio). Further, Bora, Brekke, and Powers (1994), who prepared one 7S/11S ratio (1.8) from purified fractions, reported that vicilin-rich samples had good gelling properties, while legumin formed weak gel structures. On the other hand, O'Kane, Happe, Vereijken, Gruppen, and Van Boekel (2004a) prepared three 7S/11S ratios (0.22, 0.57, and 1.2) and found that legumin formed thermally induced gels, while certain vicilin subunits inhibited gelation.

Because of these contradictory findings, the impact of pea protein profile on functional behavior remains unclear. Therefore, characterization of pea 7S vicilin, 11S legumin, and their ratios, beyond what has been reported thus far, is needed. Furthermore, the current knowledge of 11S legumin functionality has largely been acquired based on its isolated and purified form, where no studies have evaluated the functional effects of enriching a pea protein isolate with 11S legumin. Such investigation is necessary to understand how the inherent components and environmental factors introduced by the original pea protein matrix affect the protein-protein interactions and resultant functional behavior of 11S legumin in varying abundance. Furthermore, the intrinsic variance in amino acid composition of pea 7S vicilin and 11S legumin necessitates more evidence relating pea protein profile with nutritional quality. This knowledge is critical to address the lower and inconsistent nutritional quality of pea protein compared to soy protein.

The aforementioned variability in pea protein and its functionality, which goes beyond differences in protein extraction and processing conditions, continues to present formulation and consistency challenges. To successfully incorporate pea protein into different food and beverage applications and limit inconsistencies, differences in the protein profile and the consequent impact on functionality need a holistic investigation. Outcomes of a thorough investigation may also contribute to targeted breeding strategies for the continual development of pea as a source of functional and nutritious protein. Therefore, the objectives of this work were to 1) produce enriched fractions of 7S vicilin and 11S legumin from pea flour; and 2) determine the impact of each fraction and selected ratios, in the isolated form and in the native pea protein matrix, on the structural, functional, and nutritional quality of pea protein.

2. Materials and methods

2.1. Materials

Yellow pea flour was provided by AGT Foods (Regina, SK, Canada). Commercial pea protein isolate (cPPI, ProFam® Pea 580) and commercial soy protein isolate (cSPI, ProFam® 974) were provided by Archer Daniels Midland (ADM) (Decatur, IL, USA). The Dumas method (AOAC 990.03) was used to determine the protein purity of cPPI (79.5%) and of cSPI (90.7%), using a LECO® FP828 nitrogen analyzer (LECO, St. Joseph, MI, USA) and a conversion factor of 6.25. cSPI was used as a reference for certain structural and functional characteristics in comparison to pea protein samples. When not in use, samples were stored at −20 °C. Criterion™ TGX™ 4–20% precast gels, Laemmli sample buffer, 10X Tris/Glycine/sodium dodecyl sulfate (SDS) running buffer, Imperial™ Protein Stain, and Precision Plus Protein™ molecular weight (MW) marker were purchased from Bio-Rad Laboratories, Inc. (Hercules, CA, USA). A Superdex™ 200 Increase 10/300 GL Prepacked Tricorn™ Column, gel filtration low molecular weight (LMW) calibration kit, and gel filtration high molecular weight (HMW) calibration kit for size-exclusion high performance liquid chromatography (SE-HPLC) were purchased from Cytiva (Marlborough, MA, USA). A BioSuite DEAE AXC, 1000 Å column for anion exchange high performance liquid chromatography (AXC-HPLC) was purchased from Waters Corporation (Milford, MA, USA). For amino acid analysis, a Waters Acquity ultra performance liquid chromatography ethylene bridged hybrid (UPLC-BEH) C18 column (ACCQ-TAG ULTRA C18 100), AccQ Tag Ultra eluents A and B, 6-aminoquinolyl-*N*-hydroxysuccinimidylcarbamate (AQC), and Amino Acid Standard H mixture were provided by Waters (Milford, MA, USA). L-Tryptophan (Trp) and L-Norvaline (Nval) were purchased from Sigma-Aldrich (St. Louis, MO, USA). A Protein Digestibility Assay Kit (K-PDCAAS) was purchased from Megazyme International Co. (Bray, Ireland).

2.2. Production of pea protein isolate (PPI)

Native pea protein isolate (nPPI) was extracted and purified following the pH extraction method described by Hansen, Bu, and Ismail (2022). The Dumas method (AOAC 990.03) was used to determine the protein purity of nPPI (86%), using a LECO® FP828 nitrogen analyzer (LECO, St. Joseph, MI, USA) and a conversion factor of 6.25.

2.3. Production of 7S vicilin and 11S legumin enriched fractions

Commercial pea flour was fractionated into 7S vicilin and 11S legumin enriched fractions (Fig. S1 in supplementary materials) following a procedure described by Suchkov, Popello, Grinberg, and Tolstoguzov (1990) with modifications. Pea flour (180 g) was fully dispersed in a tenfold volume of double distilled water (DDW) and adjusted to pH 8.0 with 2 N NaOH. The suspension was stirred for 1 h at 50 °C and then centrifuged (5000×*g*, 30 min) to separate insoluble materials. Sodium chloride (NaCl) was added to the supernatant to reach 0.5 M, and the solution was stirred until NaCl was completely dissolved. The pH was adjusted to 4.8 using 2 N HCl, and the suspension was centrifuged (5000×*g*, 30 min) to isolate globulin proteins. The supernatant was diluted with DDW to 0.3 M NaCl and centrifuged (1000×*g*, 10 min) to separate 7S vicilin (supernatant) from 11S legumin (pellet). The 7S vicilin-containing supernatant was cooled to 5 °C and maintained at this temperature overnight. The solution was centrifuged (1000×*g*, 15 min, 5 °C), and the supernatant was diluted to 0.15 M NaCl with 5 °C DDW. The solution was centrifuged (1000×*g*, 15 min), and the precipitate collected as the 7S vicilin enriched fraction, which was suspended in DDW (1:5 w/v), neutralized (pH 7.0), dialyzed (3.5 kDa cut off), and lyophilized. The 11S legumin-containing pellet was fully dispersed in a tenfold volume of 0.6 M NaCl and centrifuged (5000×*g*, 30 min). The supernatant was diluted to 0.3 M NaCl with DDW and left overnight at room temperature. The precipitate formed was collected as the 11S legumin enriched fraction and then suspended in DDW (1:5 w/v), neutralized, dialyzed, and lyophilized. The protein content of the enriched fractions (7S vicilin: 100%; 11S legumin: 100%, data not shown) was determined by the Dumas method with a conversion factor

of 6.25. The recovery rate (g protein/g protein in the starting flour) was 9.04% for the 7S fraction and 4.64% for the 11S fraction. The fractionation was repeated approximately 60 times to obtain sufficient sample for analysis. When not in use, the samples were stored at −20 °C.

2.4. Evaluation of the effectiveness of 7S vicilin and 11S legumin fractionation

2.4.1. Protein profiling by SDS-PAGE

The protein subunit distribution in the 7S vicilin and 11S legumin enriched fractions was visualized using SDS polyacrylamide gel electrophoresis (SDS-PAGE), under reducing and non-reducing conditions, as described by Boyle, Hansen, Hinnenkamp, and Ismail (2018). All samples were loaded at equal protein amount (50 μg protein in 5 μL). The protein profile of each enriched fraction was compared to previous reports for pea vicilin and pea legumin subunit distribution (Casey & Domoney, 1999; Matta, Gatehouse, & Boulter, 1981) to verify the efficiency of 7S vicilin and 11S legumin fractionation.

2.4.2. Size-exclusion high performance liquid chromatography (SE-HPLC)

The protein components in the enriched fractions were also evaluated by size-exclusion high performance chromatography (SE-HPLC). A Shimadzu HPLC system (Shimadzu Scientific Instruments, Colombia, MD, USA) equipped with Superdex 200 Increase 10/300 GL Tricorn™ (10 × 300 mm) column, SIL-10AF auto injector, LC-20AT pump system, CTO-20A column oven, SPD-M20A photo diode array detector, and a CBM-20A communication module was used to separate proteins based on molecular weight. The analysis was performed following the method reported by Bruckner-Guhmann, Heiden-Hecht, Sozer, and Drusch (2018) and modified by Bu, Nayak, Bruggeman, Annor, and Ismail (2022). Samples (1% protein concentration, w/v) were solubilized in either pH 7 phosphate buffer (0.05 M sodium phosphate with 0.1 M sodium chloride), phosphate buffer + 0.1% SDS, or phosphate buffer + 0.1% SDS + 2.5% Beta-mercaptoethanol (BME), under magnetic agitation (250 rpm) for 2 h at room temperature. Samples were passed through a 0.45 μm polyvinylidene difluoride membrane filter, injected (100 μL), and separated isocratically using pH 7 phosphate buffer mobile phase at a flow rate of 0.5 mL per minute for a total run time of 60 min. Detection and analysis were performed at 280 nm. Molecular weights were calculated by running gel filtration calibration standards (HMW and LMW kits). Relative peak areas (the ratio of the area of a single peak to total peak area for a sample) were used to monitor differences in molecular weight distribution among the samples. Peak identities were assigned based on reported molecular weights: soluble aggregates, >450 kDa; legumin, ~450 kDa; convicilin, ~250 kDa; vicilin, ~160 kDa (Barac et al., 2010; Gatehouse, Lycett, Croy, & Boulter, 1982; Tzitzikas et al., 2006).

2.4.3. Anion exchange high performance chromatography (AXC-HPLC)

To further evaluate their protein constituents, the enriched fractions were subjected to weak AXC-HPLC using the same Shimadzu system described in section 2.4.2 but equipped with a Waters - BioSuite DEAE AXC, 1000 Å, 10 μm 7.5 × 75 mm column. Proteins were separated based on the method described by Gueguen, Vu, and Schaeffer (1984), with modifications. Samples (5% protein concentration, w/v) were solubilized in pH 7 phosphate-citrate (0.16 M) under magnetic agitation (250 rpm) for 2 h at room temperature. Samples were passed through a 0.45 μm filter, injected (100 μL), and separated following a gradient elution at a flow rate of 0.35 mL/min. From 0 to 5 min the mobile phase was held at 0 M NaCl, followed by a linear increase to 0.5 M NaCl from 5 to 10 min, then held at 0.5 M NaCl from 10 to 15 min, followed by a linear decrease to 0 M NaCl from 15 to 20 min, and finally column equilibration at 0 M NaCl from 20 to 40 min. Detection and analysis were performed at 280 nm. Peak identities were assigned based on Gueguen et al. (1984).

2.5. Production of protein isolates with differing 7S vicilin to 11S legumin ratios

2.5.1. Reconstituted protein isolates

Aliquots of the 7S vicilin and 11S legumin enriched fractions were coded as 100V and 100L, respectively, and reserved for analysis. The letter "V" (vicilin) represented the 7S vicilin enriched fraction, and the letter "L" (legumin) represented the 11S legumin enriched fraction. The remaining enriched fractions were then blended with mortar and pestle to generate three samples with differing protein ratios: 80V-20L, 50V-50L, and 20V-80L. Each sample was coded relative to its % composition of enriched fractions on a weight basis.

2.5.2. Legumin-enriched nPPI

To estimate the 7S/11S ratio in nPPI, its protein profile was evaluated, in triplicate, by SDS-PAGE/densitometry. SDS-PAGE was performed following the method described in section 2.4.1. The different bands under non-reducing conditions were assigned to legumin, vicilin, and convicilin according to their molecular weights, and their respective intensities were determined (Tzitzikas et al., 2006) using the Molecular Imager Gel Doc XR system (Bio-Rad Laboratories) with Quantity One software (version 4.6.7). The 7S/11S ratio was determined using only the bands associated with legumin and vicilin. Convicilin was not included in the ratio calculation due to its relatively low abundance in pea protein and to be consistent with previous work (Lam, Warkentin, Tyler, & Nickerson, 2017). nPPI was determined to have a 7S vicilin to 11S legumin ratio of 80:20 (data not shown). Therefore, nPPI-50LE and nPPI-80LE were produced by addition of the 11S legumin enriched fraction directly to nPPI to achieve 50% and 80% 11S legumin compositions (w/w), respectively. These samples were produced to evaluate the impact of higher 11S legumin ratio within the nPPI matrix, in comparison to the reconstituted isolates, on the overall structure and functionality.

2.5.3. Reconstituted protein isolates with increased salt content

100V-salt and 100L-salt were produced by the addition of NaCl to 100V and 100L, respectively, to determine the effect increased ionic strength had on the structure and function of the protein fractions. The initial ionic strength of each sample was calculated based on the ash content (as determined by dry ashing, AOAC 942.05: 100V: 2.19%; 100L: 1.61%) with the assumption that most of the salt present was residual NaCl. This assumption was made due to the use of NaCl solutions to fractionate the 7S vicilin and 11S legumin proteins, and NaCl production due to pH adjustments with NaOH and HCl (Kornet et al., 2021). Aliquots of 100V and 100L were fully dispersed in DDW and NaCl was added to reach 0.5 μ. Samples were stirred at room temperature for 4 h and lyophilized.

2.6. Protein structural characterization

2.6.1. Protein profiling and molecular weight distribution by SDS-PAGE and SE-HPLC

The protein profile of all samples except 100V-salt and 100L-salt was determined by SDS-PAGE as described in section 2.4.1. The same HPLC system and method described in section 2.4.2 was performed to determine molecular weight distribution, with a modified run time of 85 min. Molecular weights were calculated by running gel filtration calibration standards (HMW and LMW kits). Relative peak areas (the ratio of the area of a single peak to total peak area for a sample) were used to monitor differences in molecular weight distribution among the samples.

2.6.2. Protein denaturation as determined by differential scanning calorimetry (DSC)

The denaturation temperature and enthalpy of the protein fractions and isolates were analyzed in triplicate, using a Mettler DSC (Mettler

Toledo, Columbus, OH, USA), following the method outlined by Tang, Choi, and Ma (2007) and modified by Bu et al. (2022). Endothermic peaks were integrated for each replicate using the Mettler Toledo STARe Software version 11.00.

2.6.3. Protein surface properties

The spectrofluorometric method reported by Boyle et al. (2018) and modified by Bu et al. (2022) was utilized to measure, in triplicate, the surface hydrophobicity of the protein samples. A dynamic light scattering instrument (Malvern Nano Z-S Zetasizer) was used to measure, in triplicate, the zeta potential of protein samples as an indication of surface charge.

2.6.4. Attenuated total reflectance Fourier transform infrared spectroscopy (ATR-FTIR)

Protein samples were analyzed by a Fourier transform infrared spectrometer (Thermo Scientific™ Nicolet™ iS50 FTIR) (Bu et al., 2022, 2023). OMNIC® software was used to translate the ATR-FTIR spectra to transmission spectra and for background and baseline correction. Spectra were obtained in the mid-IR region (4000–700 cm^{-1}) at 2 cm^{-1} resolution with 32 scans. A background spectrum was measured at the same wavenumber and was subtracted from sample spectra. Baseline correction was done in the amide I region (1600 cm^{-1} –1700 cm^{-1}), and the major peaks in amide I were identified by the normalized second derivative using the embedded function in GraphPad (Prism 8). The secondary structures (α-helix, β-sheet, β-turn, and random coil) were assigned according to Sadat and Joye (2020) and Housmans et al. (2022).

2.7. Protein functional characterization

2.7.1. Protein solubility

The protein solubility of the samples, prepared at 5% protein concertation (w/v), was measured, in triplicate, following the procedure described by Wang and Ismail (2012), at pH 3.4 and pH 7, with and without heating at 80 °C for 30 min. Protein solubility was taken as the proportion of soluble protein to the total protein present in the initial solution as determined by the Dumas method.

2.7.2. Gel strength

Thermally induced gels (15 or 20% protein concentration, w/v, 95 °C for 30 min at pH 7.0) were prepared, in triplicate, as outlined by Bu et al. (2022). Samples were cooled to room temperature and a TA-TX Plus Texture Analyzer (Stable Micro Systems LTD, Surrey, UK) equipped with a 100 mm diameter probe with a test speed of 1 mm s^{-1} and distance of 0.5 mm from the plate was used to rupture the gel. The force (N) required for rupture was reported as gel strength.

2.7.3. Emulsification capacity

The emulsification capacity (EC) of protein samples (1 and 2% protein concentration, w/v) was determined, in triplicate, following the method outlined by Boyle et al. (2018) and modified by Hinnenkamp and Ismail (2021). EC was expressed as g of oil emulsified by one g of protein.

2.8. Protein digestibility – corrected amino acid score (PDCAAS)

2.8.1. Amino acid analysis

The amino acid profile of all PPIs, except 100V-salt and 100L-salt, was determined in duplicate. Cysteine and methionine were quantified following AOAC 994.12, while the remaining amino acid profile was determined following the acidic and alkaline digestion methods outlined by Temtrirath (2022) and La Cour, Jorgensen, and Schjoerring (2019), respectively, with modifications. Samples were subjected to acid digestion in a microwave digestion unit (Mars 6, CEM, NC, USA) at 155 °C for 15 min, and to alkaline digestion in a preheated conventional oven at 110 °C for 20 h. NVal (50 mM) was used as the internal standard (IS) for both acid and base digestion. Samples were then subjected to a pre-column derivatization using AQC at 55 °C for 10 min as outlined by Temtrirath (2022). Amino Acid Standard H mixture (1–100 pmol) was simultaneously prepared and derivatized following manufacturer instructions. Amino acid composition was determined following the methods of Ma et al. (2018) and Temtrirath (2022) using a Waters ACQUITY UPLC H-class system (Waters Corporation, Milford, MA, USA) equipped with a Waters Acquity UPLC-BEH C18 column (100 mm × 2.1 mm, with 1.7 μm particle size), a quaternary solvent manager (QSM), a sample manager with a Flow-Through Needle (FTN), a column oven (CH-A), and a photodiode array (PDA) detector. Amino acid peaks were integrated at 260 nm, identified based on the retention times of the corresponding standards, and quantified based on calibration curves. Integration and data processing were done using Empower 3 Software (Waters Corporation, Milford, MA, USA).

2.8.2. Protein digestibility

In vitro protein digestibility of pea protein samples, except 100V-salt and 100L-salt, was determined in duplicate using the K-PDCAAS Megazyme kit and the provided instructions. PDCAAS was then calculated as follows:

$$PDCAAS = amino\ acid\ score\ of\ first\ limiting\ amino\ acid \times true\ digestibilit\ y,$$ where

$$amino\ acid\ score\ (AAS) = \frac{First\ limiting\ amino\ acid\ content\ of\ test\ protein}{First\ limiting\ amino\ acid\ content\ in\ reference\ amino\ acid\ pattern}$$

where the reference amino acid pattern is that required for children (6 months–3 years) as defined by FAO/WHO Expert Consultation (1991).

2.9. Statistical analysis

IBM SPSS Statistics software version 27.0 for Windows (SPSS Inc., Chicago, IL, USA) was used to perform analysis of variance (ANOVA) and t-tests. Tukey-Kramer Honest Significant Difference (HSD) multiple means comparison test was used to determine significant differences ($P \leq 0.05$) among the means. Two-sample, unpaired *t*-test was used to determine significant differences ($P \leq 0.05$) between the means of two different samples.

3. Results and discussion

3.1. Effectiveness of 7S vicilin and 11S legumin fractionation

3.1.1. Protein profile of isolated fractions

The protein profiles of 100V and 100L were visualized by SDS-PAGE (Fig. 1 A and 1B, lanes 4 and 10) to assess the effectiveness of the employed fractionation. In 100V, protein bands corresponding to convicilin (~70 kDa), vicilin (~47 kDa), and vicilin fragments (~30–36 kDa, ~15–19 kDa), as identified based on previous reports (Tzitzikas

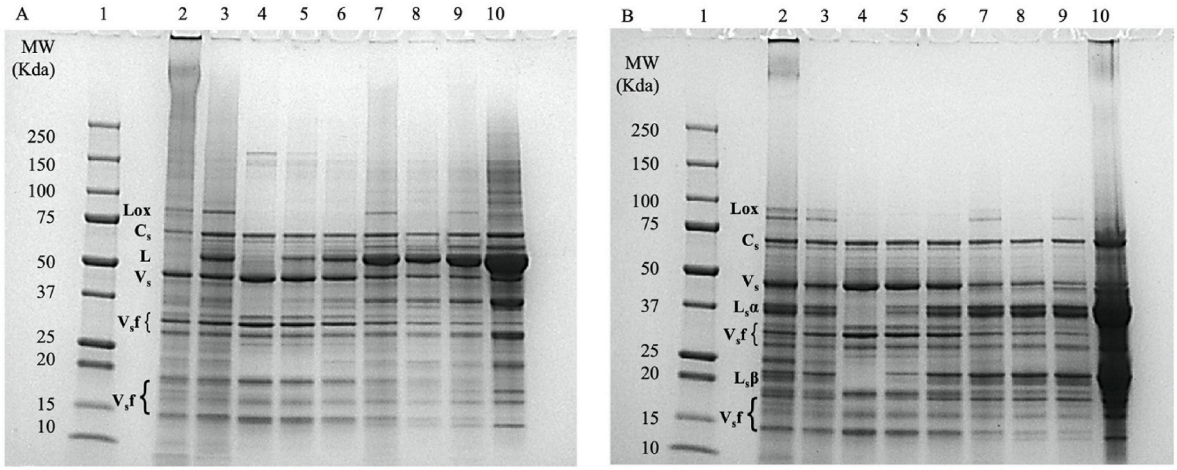

Fig. 1. SDS-PAGE gel visualization of the protein profiles of the different protein fractions and mixtures under (A) non-reducing and (B) reducing conditions. Lane 1: molecular weight standard; lane 2: cPPI; lane 3: nPPI; lane 4: 100V; lane 5: 80V-20L; lane 6: 50V-50L; lane 7: nPPI-50LE; lane 8: 20V-80L; lane 9: nPPI-80LE; lane 10: 100L. Lox: lipoxygenase; Cs: subunits of convicilin; Vs: subunits of vicilin; Lsα: acidic peptides cleaved from legumin subunits; Lsβ: basic peptide cleavage from legumin subunit; Vsf: fractions of vicilin subunits result from post-translational cleavages.

et al., 2006), were noted under non-reducing and reducing conditions (Fig. 1, lane 4). A couple of faint bands corresponding to large molecular weight polymers (~150–200 kDa) were observed under non-reducing conditions, but were not apparent under reducing conditions, indicating involvement of disulfide linkages. These polymers could potentially be residual legumin, as the shifts in pH levels and ionic strengths during fractionation might have caused residual legumin to dissociate/associate into a mixture of trimers and/or dimers (Barac, Pesic, Stanojevic, Kostic, & Cabrilo, 2015).

The bands corresponding to vicilin were darker in intensity in 100V compared to counterparts in nPPI (Fig. 1, lanes 3–4). On the other hand, individual legumin bands (~60 kDa under non-reducing conditions, ~40 and ~20 kDa under reducing conditions; Tzitzikas et al., 2006) were not visible in 100V (Fig. 1A and B, lane 4). These observations confirmed that, relative to nPPI, 100V was enriched with 7S vicilin and had negligible 11S legumin. Meanwhile, 100L had prominent legumin bands, much darker in intensity than their counterparts in nPPI (Fig. 1A and B, lanes 3 and 10). This observation confirmed that 100L was enriched with 11S legumin relative to nPPI. A greater abundance of large molecular weight polymers, as indicated by dark smearing in the

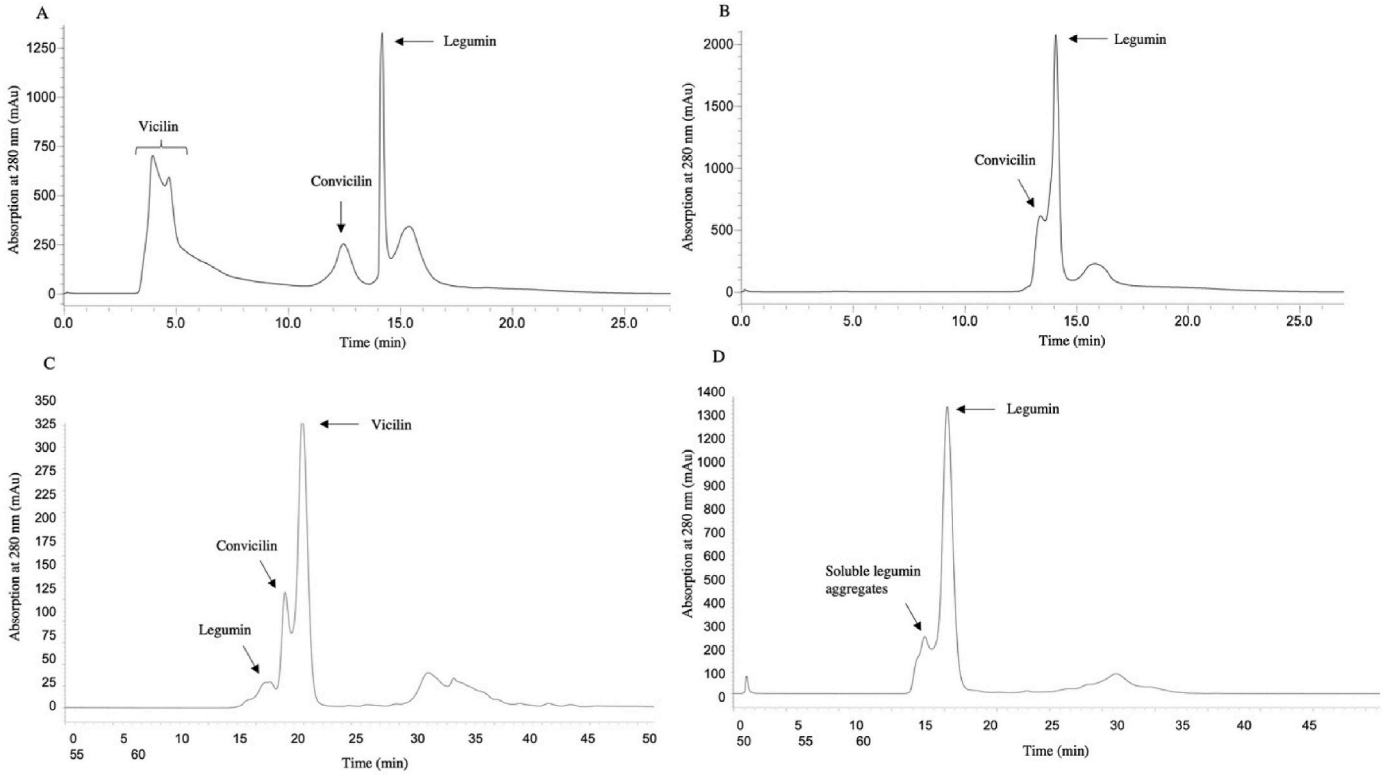

Fig. 2. Visualization of the distribution of protein components in the enriched fractions by anion-exchange chromatography (AXC) and size-exclusion chromatography (SEC). Chromatogram (A) 7S vicilin enriched fraction under AXC, (B) 11S legumin enriched fraction under AXC, (C) 7S vicilin enriched fraction under SEC, (D) 11S legumin enriched fraction under SEC.

upper region of the lane, were noted in 100L compared to 100V (Fig. 1A, lane 10 compared to lane 4). Presence of these polymers was likely induced by the additional changes in extraction conditions to isolate the 11S legumin fraction, as discussed. Changes in pH, temperature, and ionic strength can alter protein conformation by disrupting electrostatic and hydrophobic forces, inducing denaturation and subsequent polymerization (Damodaran & Parkin, 2017). Under reducing conditions, smearing in the upper region of 100L's lane was reduced yet was still apparent, indicating the involvement of covalent bonds beyond disulfide linkages (Fig. 1B, lane 10).

Protein bands corresponding to convicilin and vicilin were also observed in 100L (Fig. 1A and B, lane 10). Contamination of convicilin and various vicilin subunits in an isolated legumin fraction has been previously reported (Bora et al., 1994; Koyoro & Powers, 1987; Mession, Assifaoui, Cayot, & Saurel, 2012; Mession, Chihi, Sok, & Saurel, 2015; O'Kane et al., 2004a).

3.1.2. Purity of the protein fractions

To further determine the effectiveness of fractionation, the purity of the 7S vicilin and 11S legumin enriched fractions was evaluated by AXC and SE-HPLC (Fig. 2). Following AXC, chromatographic peaks corresponding to vicilin, convicilin, and legumin were identified within the 7S vicilin enriched fraction (Fig. 2A) based on the elution patterns reported by Gueguen et al. (1984). The sensitivity of the UV detection confirmed the presence of residual 11S legumin within the 7S vicilin enriched fraction, while protein bands corresponding to legumin were not visible by SDS-PAGE (Fig. 1). The combined observations indicated that the 11S legumin contamination might not have been quantitatively significant. Meanwhile, one prominent, high intensity chromatographic peak corresponding to legumin was identified within the 11S legumin enriched fraction (Fig. 2B). A minor/low intensity peak was identified as residual convicilin (Gueguen et al., 1984), corroborating the presence of its corresponding protein band (Fig. 1).

Similarly, three chromatographic peaks (Fig. 2C) were identified within the 7S vicilin enriched fraction by SE-HPLC as legumin, convicilin, and vicilin, based on previously reported elution patterns (Gatehouse et al., 1982). The legumin peak had a relatively low intensity compared to that of vicilin, confirming the residual presence of 11S legumin in the 7S vicilin enriched fraction, as discussed. On the other hand, a high intensity chromatographic peak corresponding to legumin was identified in the 11S legumin enriched fraction (Fig. 2D). Another low-intensity chromatographic peak was also noted in the 11S legumin enriched fraction, potentially corresponding to dimers and/or trimers of legumin. While both AXC and SE-HPLC revealed contamination in the 7S vicilin and 11S legumin enriched, residual counterparts were present in relatively low proportions. Although similar findings prompted some researchers to use chromatography to further purify the crude fractions, purification had very low yield and was time consuming, limiting the extent of structural and functional characterization of the isolates (Bora et al., 1994; Koyoro & Powers, 1987; O'Kane et al., 2004a). Further, Bora et al. (1994) reported there was no functional difference between crude and purified legumin fractions. Therefore, in this study, characterization of crude fractions, rather than purified ones, was chosen to fill knowledge gaps regarding pea 7S vicilin, 11S legumin, and their ratios.

3.2. Structural properties of the isolated fractions, reconstituted protein isolates, and legumin-enriched nPPIs

3.2.1. Protein profile and molecular weight distribution

The protein profiles of the reconstituted protein isolates and legumin-enriched nPPIs were consistent with the targeted 7S/11S ratios (Fig. 1). Under non-reducing conditions, the intensity of the legumin band (~60 kDa) increased following its increasing abundance across 80V-20L, 50V-50L, 20V-80L, and 100L (Fig. 1, lanes 5–10). Meanwhile, the intensity of vicilin bands (~45, 30–36, 15–19 kDa) progressively decreased across 100V, 80V-20L, 50V-50L, 20V-80L, and 100L, which affirmed decreasing vicilin abundance. These legumin and vicilin patterns were similar among the samples under reducing conditions, though the former was exhibited in its subunits (~40 kDa and 20 kDa) rather than in the monomer form (~60 kDa).

Dark smearing in the upper portion of the lanes was especially evident in cPPI, nPPI, and 100L under non-reducing conditions (Fig. 1A, lanes 2, 3, 10). Such smearing was also noted, albeit less intense, in nPPI-50LE and nPPI-80LE (Fig. 1A, lanes 7 and 9). 100V, 80V-20L, 50V-50L, and 20V-80L exhibited the least smearing among the samples (Fig. 1A, lanes 4, 5, 6, 8). Under reducing conditions, the noted smearing was reduced (Fig. 1B), which indicated that all the mentioned isolates contained disulfide-linked polymers to certain extents. However, residual smearing was noted in cPPI and 100L lanes under reducing conditions, which indicated protein polymerization via covalent bonding beyond disulfide linkages (Fig. 1B, lanes 2 and 10). The extent of polymerization is mostly attributed to the extraction process. The use of harsh extraction parameters to produce cPPI induced protein denaturation and subsequent polymerization (Hansen et al., 2022). Meanwhile, the fractionation conditions utilized in this study induced greater polymerization in the 11S legumin enriched fraction than in the 7S vicilin enriched fraction, mostly due to protein denaturation.

To further characterize the molecular weight (MW) distribution of soluble aggregates, functional proteins (legumin, vicilin, and convicilin), and low molecular weight polypeptides, samples were analyzed by SE-HPLC following solubilization in phosphate buffer, phosphate buffer + SDS, and phosphate buffer + SDS and BME (Table 1, Fig. 3). The chromatographic peaks corresponding to >450 kDa polymers were collectively identified as soluble aggregates, since they were soluble in the sample buffer and passed filtration (0.45 μm) prior to injection on the column. Chromatographic peaks corresponding to hexameric legumin, trimeric convicilin, and trimeric vicilin were identified according to their reported MW ranges (Barac et al., 2010; Gatehouse et al., 1982; Tzitzikas et al., 2006).

In phosphate buffer, cPPI had a high relative abundance of soluble aggregates but significantly ($P < 0.05$) the least functional proteins among all samples (Table 1, Fig. 3A), which complimented the SDS-PAGE observation (Fig. 1). This MW distribution indicated that most functional proteins in cPPI likely polymerized into large insoluble aggregates that did not pass through the filter (0.45 μm) and thus were not represented by a chromatographic peak. In contrast, nPPI had a significantly lower abundance of soluble aggregates than cPPI but a significantly higher percent distribution of each functional protein (Table 1). Among the reconstituted protein isolates, the abundance of soluble aggregates significantly increased with the relative proportion of 11S legumin (Table 1). Similarly, the relative abundance of soluble aggregates was significantly higher in nPPI-80LE than nPPI-50LE. This observation complemented that of the SDS-PAGE, where protein bands corresponding to high molecular weight polymers increased in intensity with higher proportion of the 11S legumin fraction. The difference in soluble aggregates among all the samples was attributed to the effects of fractionation conditions on protein structure, as discussed.

Meanwhile, the MW distribution of functional proteins in the isolated fractions, reconstituted isolates, and legumin-enriched nPPIs was consistent with the targeted 7S/11S ratios (Table 1). Relative abundance of legumin was significantly the highest in 100L and decreased following its lower abundance across nPPI-80LE, 20V-80L, nPPI-50LE, 50V-50L, 80V-20L, and 100V (Table 1). On the other hand, the relative abundance of vicilin was significantly the highest in 100V and decreased with the reduction in 7S vicilin proportion in the different samples. Convicilin was present in similar percent relative abundance in all the samples, which affirmed the contamination noted in the legumin-enriched fraction (Fig. 1), as discussed.

Noncovalent bonds were disrupted with the addition of SDS into the sample buffer, which generally increased the relative abundance of soluble aggregates, decreased that of hexameric and trimeric functional proteins, and slightly increased that of lower MW polypeptides among

Table 1
Molecular weight and relative abundance of soluble aggregates, legumin, convicilin, and vicilin present in cPPI, nPPI, isolated fractions, reconstituted protein isolates, and legumin-enriched nPPIs with varying 7S vicilin to 11S legumin ratios as analyzed by size-exclusion high-performance liquid chromatography (SE-HPLC).

Sample	Relative Abundance (%) of Protein Fractions[a]											
	Phosphate Buffer[b]				Phosphate Buffer (0.1% SDS)[c]				Phosphate Buffer (0.1% SDS+ 2.5% BME)[d]			
	Soluble aggregates (>450 kDa)	Legumin (384–446 kDa)	Conviclin (252–296 kDa)	Vicilin (167–181 kDa)	Soluble aggregates	Legumin	Conviclin	Vicilin	Soluble aggregates	Legumin	Conviclin	Vicilin
cPPI	21.7 ± 0.18[ae]	2.20 ± 0.00[h]	6.15 ± 0.02[b]	4.93 ± 0.05[f]	20.5 ± 0.25[c]	4.89 ± 0.02[h]	6.23 ± 0.07[c]	4.84 ± 0.05[g]	33.0 ± 0.63[a]	2.46 ± 0.06[f]	6.69 ± 0.04[bc]	3.46 ± 0.07[ef]
nPPI	4.55 ± 0.33[b]	20.7 ± 0.02[e]	8.49 ± 0.01[a]	11.8 ± 0.07[d]	11.4 ± 0.96[e]	16.9 ± 0.11[f]	8.48 ± 0.03[a]	12.4 ± 0.10[d]	17.5 ± 0.28[e]	17.4 ± 0.08[d]	7.72 ± 0.03[ab]	11.1 ± 0.10[cd]
100V	2.01 ± 0.00[b]	5.08 ± 0.07[g]	4.44 ± 0.21[d]	48.3 ± 0.14[a]	2.40 ± 0.00[g]	3.02 ± 0.07[i]	5.32 ± 0.11[d]	47.5 ± 0.08[a]	2.20 ± 0.16[g]	3.06 ± 0.26[f]	8.76 ± 0.86[a]	36.4 ± 2.30[a]
80V-20L	6.76 ± 1.44[b]	17.7 ± 0.84[f]	7.81 ± 0.92[b]	30.9 ± 0.15[b]	9.06 ± 0.06[f]	10.7 ± 0.01[g]	7.35 ± 0.12[b]	32.1 ± 0.09[b]	8.45 ± 0.08[f]	12.7 ± 0.04[e]	7.98 ± 0.19[ab]	27.4 ± 0.02[b]
50V-50L	17.5 ± 0.16[a]	28.9 ± 0.12[d]	5.65 ± 0.02[bc]	16.5 ± 0.05[c]	21.2 ± 0.52[c]	26.1 ± 0.36[d]	5.77 ± 0.05[cd]	7.81 ± 0.08[f]	21.6 ± 0.32[cd]	25.3 ± 0.01[b]	5.08 ± 0.05[cd]	7.27 ± 0.04[de]
nPPI-50LE	6.48 ± 0.60[b]	31.4 ± 0.06[c]	6.06 ± 0.06[b]	7.36 ± 0.02[e]	17.4 ± 0.04[d]	20.4 ± 0.30[e]	3.62 ± 0.34[fg]	18.5 ± 0.38[c]	15.7 ± 0.13[e]	22.4 ± 0.19[c]	6.37 ± 0.00[bc]	15.0 ± 0.12[c]
20V-80L	21.3 ± 0.34[a]	36.9 ± 0.42[b]	5.33 ± 0.08[bcd]	8.17 ± 0.11[e]	26.3 ± 0.04[a]	30.3 ± 0.18[b]	4.52 ± 0.02[e]	5.29 ± 0.03[g]	21.2 ± 0.29[d]	30.2 ± 0.80[a]	4.44 ± 0.26[d]	7.86 ± 0.52[de]
nPPI-80LE	17.6 ± 1.36[a]	37.9 ± 0.37[b]	4.51 ± 0.10[cd]	4.56 ± 0.16[f]	24.2 ± 0.07[b]	28.7 ± 0.06[c]	4.33 ± 0.05[ef]	9.00 ± 0.01[e]	25.1 ± 0.78[b]	29.9 ± 0.14[a]	3.51 ± 0.03[de]	4.40 ± 0.51[ef]
100L	22.2 ± 1.23[a]	42.4 ± 0.31[a]	4.48 ± 0.02[d]	1.28 ± 0.10[g]	28.3 ± 0.08[a]	33.0 ± 0.09[a]	3.15 ± 0.02[g]	2.00 ± 0.01[h]	23.7 ± 0.15[bc]	30.9 ± 0.04[a]	2.63 ± 0.05[e]	2.30 ± 0.10[f]

[a] Relative abundance (%) is the area of a specific peak divided by the total peak area for that sample.
[b] Samples were dissolved in pH 7 phosphate buffer.
[c] Samples were dissolved in pH 7 phosphate buffer with the presence of 0.1% SDS.
[d] Samples were dissolved in pH 7 phosphate buffer with the presence of 0.1% SDS and 2.5% BME.
[e] Lowercase letters indicate significant differences among the means (n = 2) in each column, according to the Tukey-Kramer multiple means comparison test ($P < 0.05$).

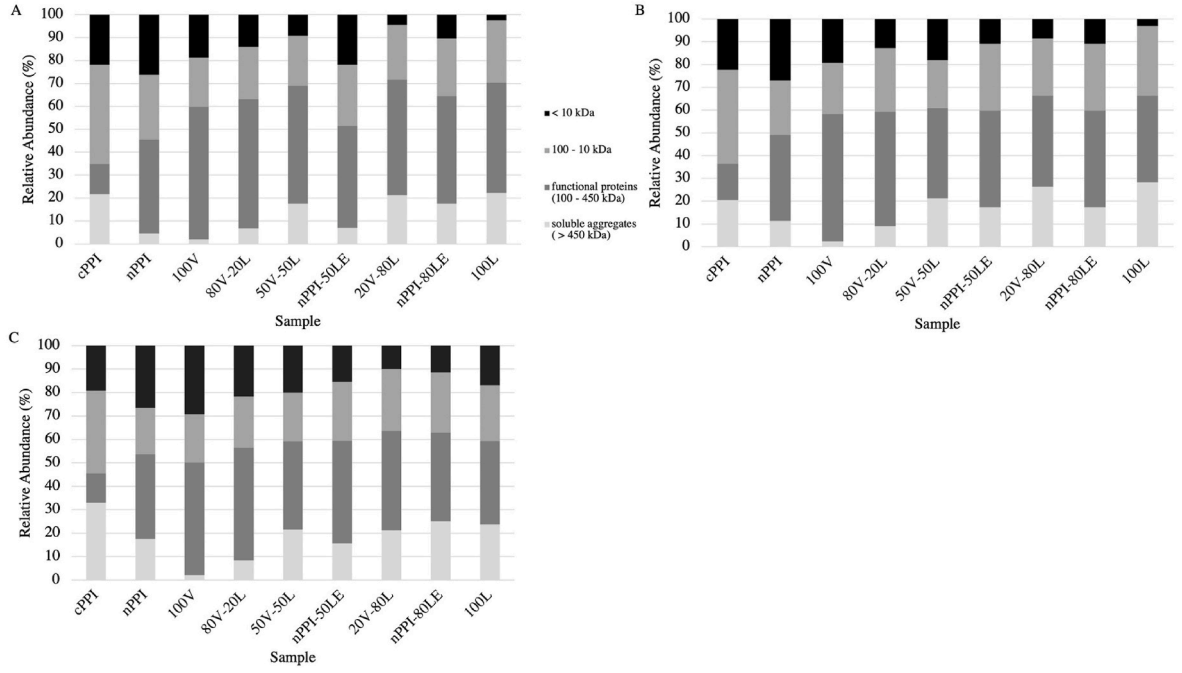

Fig. 3. Percent relative abundance of different protein fractions in cPPI, nPPI, isolated fractions, reconstituted protein isolates, and legumin-enriched nPPIs. Samples were dissolved in (A) pH 7 phosphate buffer, (B) pH 7 phosphate buffer with 0.1% SDS, and (C) pH 7 phosphate buffer with 0.1% SDS and 2.5% BME, and analyzed by SE-HPLC. Bars distribution represents means of n = 2.

the samples (Table 1, Fig. 3B). The addition of BME would cleave disulfide linkages, potentially increasing the relative abundance of soluble aggregates, legumin, and low MW polypeptides, while simultaneously decreasing the abundance of legumin monomers due to their reduction into acidic and basic subunits. Indeed, both cPPI and nPPI exhibited a significantly ($P < 0.05$) higher relative abundance of soluble aggregates when solubilized in the presence of BME (Table 1, Fig. 3C compared to 3A). However, the relative abundance of legumin and low MW polypeptides in cPPI and nPPI was hardly affected by the addition of BME. The partial dissociation of insoluble aggregates and soluble aggregates in the presence of BME masked the potential reduction of monomeric legumin into its low MW subunits, resulting in no observed change in the percent relative abundance. On the other hand, a significantly ($P < 0.05$) higher relative abundance of low MW polypeptides was observed across the isolated fractions, reconstituted isolates, and legumin-enriched nPPIs (Fig. 3C compared to 3A). However, the percent relative abundance of soluble aggregates and functional proteins was hardly affected in these samples (Table 1). This observation could be partially attributed to low abundance of insoluble aggregates in these samples compared to cPPI and nPPI. In addition, reduction of disulfide linkages could have been incomplete due to inaccessible disulfide bonds buried within large, polymerized proteins, especially in 100L and 20V-80L. Both of these samples had negligible changes in soluble aggregates under SDS and BME relative to the phosphate buffer alone (Table 1). The presence of these compact, polymerized proteins may limit protein functionality.

3.2.2. Protein denaturation state

Discrepancies in the reported thermal stability of pea protein have been partially attributed to intrinsic determinants such as protein profile and environmental conditions (Mession et al., 2015). Therefore, in this study, the impact of 7S/11S ratio and salt on protein denaturation temperature and enthalpy were evaluated.

Apart from cSPI and cPPI, which were already denatured and thus lacked a thermal transition (Bu et al., 2022, 2023), and apart from nPPI that had two overlapping endothermic peaks, the remaining samples had one prominent endothermic peak. In the latter case, the two peaks were integrated as one due to the intersecting transition temperatures for 7S and 11S globulins (Mession et al., 2012). While the denaturation temperatures and enthalpies of the reconstituted isolates and legumin-enriched nPPIs were similar to previous reports on pea protein (Bu et al., 2022; Hansen et al., 2022; Kornet et al., 2021), those of 100V-salt and 100L-salt were significantly higher (Table 2). The latter observation was attributed to the stabilizing effect of NaCl on protein structure (Sun & Arntfield, 2010, 2012).

Among nPPI, nPPI-50LE, and nPPI-80LE, denaturation temperature and enthalpy increased with the relative abundance of 11S legumin. Legumin's thermal stability is attributed to its complex quaternary structure and intermolecular disulfide bridges, which require relatively high energy to disrupt (Mession et al., 2015). Further, when added to nPPI in high concentrations, the partially denatured isolated legumin fraction potentially induced a hydrophobicity driven protein association (Fig. 1), stabilized by both hydrophobic and disulfide interactions (Rickert, Johnson, & Murphy, 2004). Thus, nPPI-80LE's enthalpy of denaturation was significantly higher than that of nPPI-50LE and nPPI (Table 2).

Meanwhile, the isolated fractions and their corresponding reconstituted isolates had lower enthalpies of denaturation than nPPI and the legumin-enriched nPPIs. This finding was attributed to the partial denaturation that occurred during the extraction, as discussed. These differences in denaturation state among the samples will likely contribute to differences in other structural and in functional properties.

3.2.3. Protein surface properties

Although nonpolar residues typically inhabit ~40–50% of the water-accessible surface for most globular plant proteins, the ratio and distribution of polar to nonpolar regions are partially dictated by protein profile as well as amino acid composition and sequence (Damodaran & Parkin, 2017). The unique sequence of amino acids lining the protein's surface partially determines its overall surface hydrophobicity and charge, which will in turn affect functional behavior. Therefore, the impact of 7S/11S ratio and salt on surface properties were evaluated for all of the pea protein samples in reference to cSPI.

cSPI and cPPI had significantly the highest surface hydrophobicity, which complimented the observed denaturation data (Table 2), similar to previous reports (Bu et al., 2022; Hansen et al., 2022). Intramolecular electrostatic interactions, hydrogen bonding, and hydrophobic interactions that stabilize the protein are disrupted upon denaturation, leading to protein unfolding and exposure of the mostly hydrophobic core. Upon partial exposure of the hydrophobic core, the surface hydrophobicity is proportionally increased (Foegeding & Davis, 2011).

Among the fractionated and reconstituted isolates, 100L had the highest surface hydrophobicity, while 100V had the lowest (Table 2). This finding agreed with that of Mwasaru, Muhammad, Bakar, and Che Man (1999) and Barac et al. (2010), who reported legumin had more surface hydrophobic groups than vicilin. As previously discussed, the elaborate extraction steps and changes in their associated environmental conditions induced protein denaturation in 100L, which led to enhanced surface hydrophobicity relative to 100V. In contrast, the surface

Table 2
Denaturation temperatures and enthalpy, surface hydrophobicity, and surface charge of cSPI, cPPI, nPPI, isolated fractions, reconstituted protein isolates, and legumin-enriched nPPIs with varying 7S vicilin to 11S legumin ratios.

Sample	Denaturation Temperature and Enthalpy		Surface Properties	
	Denaturation Temperature	Enthalpy of Denaturation	Surface Hydrophobicity	Surface Charge
	Td, °C	ΔH, J g-1 protein	Net Relative Fluorescence Intensity	mV
cSPI	*[a]	*	11736 ± 196^{ab}	−41.9 ± 0.72^{a}
cPPI	*	*	10261 ± 320^{b}	−34.8 ± 0.43^{bcde}
nPPI	84.00 ± 0.18^{ef}	7.10 ± 0.13^{c}	8021 ± 228^{c}	−34.9 ± 0.40^{bcde}
100V	83.63 ± 0.50^{f}	5.32 ± 0.26^{cd}	4097 ± 189^{f}	−33.7 ± 0.50^{cde}
100V-salt	88.37 ± 0.11^{b}	14.90 ± 0.18^{a}	7177 ± 127^{cd}	−6.94 ± 0.47^{g}
80V-20L	84.88 ± 0.07^{def}	3.44 ± 0.20^{d}	5063 ± 107^{f}	−33.5 ± 0.34^{de}
50V-50L	85.38 ± 0.16^{cde}	6.30 ± 0.50^{c}	4840 ± 83.5^{f}	−33.4 ± 0.42^{e}
nPPI-50LE	85.87 ± 0.28^{cd}	7.31 ± 0.57 ^{c}	7373 ± 156^{cd}	−36.6 ± 0.38^{b}
20V-80L	85.88 ± 0.41^{cd}	3.15 ± 0.39^{d}	5685 ± 111^{ef}	−35.9 ± 1.01^{bcde}
nPPI-80LE	86.74 ± 0.24^{c}	9.83 ± 0.86^{b}	6617 ± 74.2^{de}	−36.4 ± 0.40^{bc}
100L	86.33 ± 0.39^{c}	6.14 ± 0.26^{c}	6027 ± 199^{e}	−36.1 ± 0.44^{bcd}
100L-salt	98.01 ± 0.00^{a}	15.75 ± 0.59^{a}	7610 ± 98.8^{c}	−10.2 ± 0.66^{f}

[a] An asterisk (*) denotes no peak of denaturation observed.

[b] Lowercase letters indicate significant differences among the means (n = 3) in each column, according to the Tukey-Kramer multiple means comparison test ($P < 0.05$).

hydrophobicity of nPPI and the legumin-enriched nPPIs decreased as 11S legumin abundance increased. As discussed, the isolated legumin fraction induced a hydrophobicity driven protein polymerization when added to nPPI, which subsequently reduced the surface hydrophobicity of nPPI-50LE and nPPI-80LE (Wang & Ismail, 2012). This observation emphasized the compounded effect of denaturation and 7S/11S ratio on extent of polymerization and resultant surface properties. Meanwhile, the addition of NaCl in 100V-salt and 100L-salt led to significantly higher surface hydrophobicity compared to their 100V and 100L counterparts. NaCl likely shielded some charges on the surface of the protein, leading to higher perceived hydrophobicity (Damodaran, 1988).

Zeta potential (ζ) was measured as an indication of surface charge. All samples, except 100L-salt and 100V-salt, carried a highly net negative charge at pH 7 (Table 2), which was attributed to the charge shielding effect of NaCl (Damodaran, 1988). Samples with a higher 11S legumin abundance (100L, 20V-80L, nPPI-50LE, and nPPI-80LE) had higher net negative charge than 100V, with a few minor statistical differences. Danielsson (1949) determined the isoelectric points of legumin and vicilin as pH 4.8 and 5.5, respectively. Accordingly, at pH 7, legumin is further from its isoelectric point and therefore carries a greater net negative charge than vicilin, which may explain the observed differences. The interplay of surface charge and surface hydrophobicity affect how the protein interacts with its environment, and therefore will impact functional behavior.

3.2.4. *Protein secondary structures*

The secondary structure profile of pea protein samples was deduced via the deconvolution of the Amide I peak. The secondary structure of cPPI was dominated by intermolecular β sheet (Fig. 4A). Protein unfolding and polymerization during extraction could have initiated the formation of intermolecular β sheet due to the proximity of proteins and

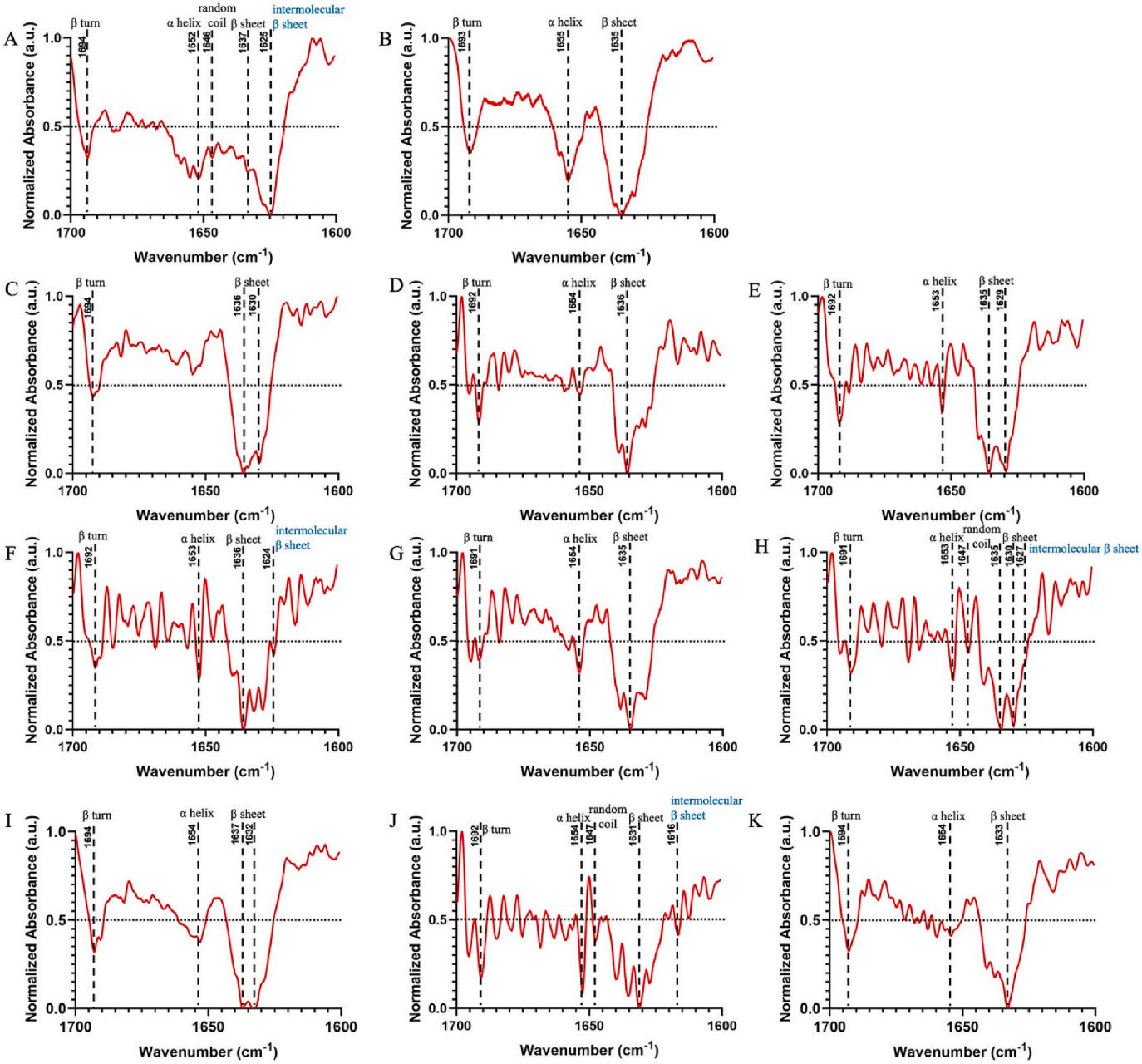

Fig. 4. The second derivative of FTIR-ATR spectra. (A) cPPI (B) nPPI (C) 100V (D) 100V-salt (E) 80V-20L (F) 50V-50L (G) nPPI-50LE (H) 20V-80L (I) nPPI-80LE (J) 100L (K) 100L-salt.

exposed amino acids residues (Bu et al., 2022). Additionally, random coil was prominent in cPPI. This could be another indication of protein denaturation, as environmental factors such as heat can induce the loss of ordered secondary structure (Marti, Bock, Pagani, Ismail, & Seetharaman, 2016). Meanwhile, the intermolecular β sheet and random coil were absent in nPPI; instead, β sheet, α helix, and β turn largely dominated the Amide I region (Fig. 4B). This finding suggested that, in contrast to cPPI, the secondary structure of nPPI was mostly preserved due to mild extraction conditions.

In comparing the isolated fractions, β sheet and β turn dominated the Amide I region of 100V, while random coil, β sheet, α helix, and intermolecular β sheet were all prominent in that of 100L (Fig. 4, C & J). This major difference in secondary structure between 100V and 100L was largely attributed to the intrinsic structural differences between vicilin and legumin (Barac et al., 2010). Further, random coil and intermolecular β sheet in 100L could be due to the fractionation process, in agreement with the SDS-PAGE observations (Fig. 1), as discussed. However, the addition of salt decreased the relative abundance of the intermolecular β sheet and random coil in 100L and increased α helix in 100V (Fig. 4, D & K). This observation indicated that the additional salt stabilized the secondary structure of vicilin and legumin, which agreed with the enhanced denaturation enthalpy of 100V-salt and 100L-salt (Table 2).

Although α helix was not detected in 100V, the reconstituted protein isolates and legumin-enriched nPPIs had an apparent α helix region, attributed to the presence of legumin (Fig. 4, E, F, G, H, & I). In addition, high abundance of legumin in reconstituted protein isolates contributed to the presence of intermolecular β sheet and random coil (Fig. 4, F & H). Legumin-enriched nPPIs (Fig. 4, G & I), on the other hand, were not largely impacted by the additional legumin, which could be attributed to the nPPI matrix effect. Protein secondary structure predominated by β sheet could be beneficial to some functional properties such as gelation and emulsification, whereas random coil and intermolecular β sheet could reduce protein solubility (Bu et al., 2022; Cao & Mezzenga, 2019; Clark, Kavanagh, & Ross-Murphy, 2001; Damodaran & Parkin, 2017; Hill, Ledward, & Mitchell, 1998; McClements & Grossmann, 2022).

3.3. Functional properties of the isolated fractions, reconstituted protein isolates, and legumin-enriched nPPIs

3.3.1. Protein solubility

Protein solubility is a critical functionality for high protein beverages as well as food applications that involve other functional properties such as thickening, foaming, emulsifying, and gelling (Damodaran & Parkin, 2017). Protein solubility is governed by intrinsic characteristics such as molecular weight and surface properties and is also influenced by environmental conditions such as pH, ionic strength, and temperature (Damodaran & Parkin, 2017; Guo, Hu, Wang, & Ai, 2017). Therefore, in this study, the impact of 7S/11S ratios and salt on protein solubility were evaluated at neutral and acidic pH and under non-heated and heated conditions.

cPPI was significantly the least soluble among the samples across all conditions (Table 3), which was partially attributed to its denatured state (Table 2) and extent of polymerization (Fig. 1). As discussed, denaturation often increases surface hydrophobicity, which will hinder protein-water interactions and decrease protein solubility. In contrast, despite its denatured state, cSPI was significantly more soluble than cPPI under neutral conditions. This finding is attributed to cSPI's significantly higher surface charge at pH 7 compared to cPPI (Table 2), which permitted sufficient protein-water interactions under neutral conditions. Further, both cSPI and cPPI had higher protein solubility under heated conditions (Table 3). When heated below the denaturation temperature, protein solubility may increase slightly due to the increase in entropy of mixing at higher temperatures (Grossmann & McClements, 2022). On the other hand, nPPI was significantly more soluble than the commercial ingredients across most conditions as it was less denatured and had lower surface hydrophobicity (Table 2).

In comparing the isolated fractions, 100V was significantly more soluble than 100L across all conditions (Table 3). This finding was partially attributed to 100V's relatively less polymerization (Fig. 1), significantly lower surface hydrophobicity, (Table 2), and lack of intermolecular β sheet and random coil compared to 100L (Fig. 4). Samples that are less polymerized are more soluble because of the more favorable entropy contribution (Grossmann & McClements, 2022). Moreover, the intrinsic properties of pea vicilin, namely its lower molecular weight, glycosylated subunits, and high flexibility, likely contributed to 100V's high solubility across all conditions (Kimura et al., 2008; Maruyama et al., 2002; Pedrosa, Trisciuzzi, & Ferreira, 1997). Further, at pH 3.4, vicilin holds a greater net positive charge than legumin due to its higher isoelectric point (5.5 vs. 4.8), which may have further enhanced its interaction with water (Danielsson, 1949).

The isolated fractions, reconstituted isolates, and legumin-enriched nPPI samples had comparable or better solubility than nPPI across all conditions, except for 80V-20L at pH 7 (Table 3). This exception cannot be explained by differences in the surface properties of 80V-20L compared to the other samples (Table 2), but instead could be related

Table 3
Solubility, gel strength and emulsification capacity of cSPI, cPPI, nPPI, isolated fractions, reconstituted protein isolates, and legumin-enriched nPPIs with varying 7S vicilin to 11S legumin ratios.

Sample	% Protein Solubility (5% protein)				Gel Strength (20% protein)	Emulsification Capacity (2% protein)
	pH 7		pH 3.4			
	Non-Heated	Heated (80 °C for 30 min)	Non-Heated	Heated (80 °C for 30 min)	Strength (N)	mL oil/g protein
cSPI	73.5 ± 2.92^{ba}	86.1 ± 3.19^{ab}	28.1 ± 0.92^{f}	38.3 ± 0.67^{f}	16.69 ± 1.13^{ab}	1102.1 ± 27.8^{ac}
cPPI	31.4 ± 0.44^{d}	54.2 ± 0.53^{e}	12.5 ± 0.09^{g}	18.0 ± 0.17^{g}	8.37 ± 0.32^{d}	725.4 ± 28.4^{b}
nPPI	85.5 ± 1.92^{a}	81.4 ± 0.32^{bc}	49.8 ± 0.45^{e}	62.4 ± 0.59^{e}	4.62 ± 0.10^{f}	502.2 ± 14.2^{efg}
100V	91.4 ± 2.93^{a}	74.9 ± 1.71^{cd}	95.4 ± 0.59^{a}	96.0 ± 0.99^{a}	13.8 ± 0.31^{b}	697.5 ± 26.8^{bc}
100V-salt	93.3 ± 0.62^{a}	73.9 ± 0.58^{cd}	75.8 ± 0.50^{cd}	6.95 ± 0.23^{h}	17.2 ± 0.18^{a}	534.8 ± 14.0^{ef}
80V-20L	63.7 ± 2.70^{c}	61.8 ± 0.75^{e}	92.3 ± 1.11^{a}	90.3 ± 2.12^{ab}	11.5 ± 0.52^{c}	589.0 ± 27.6^{cde}
50V-50L	89.8 ± 1.24^{a}	72.7 ± 1.42^{d}	83.9 ± 0.59^{b}	87.6 ± 0.18^{bc}	6.31 ± 0.14^{e}	568.9 ± 1.55^{de}
nPPI-50LE	88.6 ± 0.88^{a}	81.2 ± 1.64^{bc}	72.9 ± 1.52^{d}	78.0 ± 1.73^{d}	*^{d}	434.0 ± 21.7^{fg}
20V-80L	86.0 ± 3.48^{a}	72.8 ± 0.67^{d}	83.2 ± 1.18^{b}	88.1 ± 1.54^{bc}	2.66 ± 0.05^{g}	545.6 ± 16.4^{ef}
nPPI-80LE	92.4 ± 1.36^{a}	89.6 ± 1.55^{a}	78.0 ± 0.31^{c}	83.4 ± 0.69^{cd}	1.31 ± 0.06^{h}	393.7 ± 3.10^{g}
100L	69.7 ± 1.40^{bc}	62.0 ± 1.67^{e}	79.5 ± 0.55^{bc}	81.4 ± 2.40^{cd}	2.61 ± 0.11^{g}	130.2 ± 5.37^{h}
100L-salt	87.2 ± 1.11^{a}	85.7 ± 1.25^{ab}	49.9 ± 1.27^{e}	18.1 ± 1.07^{g}	2.26 ± 0.09^{gh}	663.4 ± 31.0^{bcd}

[a] Lowercase letters indicate significant differences among the means (n = 3) in each column, according to the Tukey-Kramer multiple means comparison test ($P < 0.05$).
[b] Gel strength was measured at 15% protein concentration for cSPI.
[c] Emulsification capacity was measured at 1% protein concentration for cSPI.
[d] An asterisk (*) denotes no gel formed at 20% protein concentration.

to possible differences in ionic strength and other unclear compounded factors. At pH 3.4 specifically, the significantly lower solubility of nPPI compared to the produced pea protein samples could be partly attributed to its significantly higher surface hydrophobicity (Table 2) and ash content (~4% vs. 2%, data not shown). The low net charge of protein at this acidic pH, coupled with high ionic strength, reduce protein solubility (Kimura et al., 2008). Therefore, at pH 3.4, the amount of salt in nPPI most likely had a charge-shielding effect on the protein and potentially competed for water, hindering protein-water interactions. This phenomenon was further demonstrated in 100V-salt and 100L-salt, as their solubility at pH 3.4 was significantly reduced compared to 100V and 100L counterparts. Further, heating 100V-salt and 100L-salt at 80 °C for 30 min drastically reduced solubility due to protein denaturation and a salting-out effect (Damadoran, 1988). The increase in thermal kinetic energy under heated conditions likely enhanced hydrophobicity-driven protein-protein interactions and exacerbated the decrease in solubility (Damodaran & Parkin, 2017).

Meanwhile, the solubility of 100V-salt was not significantly different than that of 100V under neutral conditions (Table 3), despite the former's significantly higher surface hydrophobicity and lower surface charge (Table 2). Vicilin's intrinsic structure, which favors solubility, potentially overcame the environmental effects imposed by salt to remain highly soluble under neutral pH. A similar phenomenon has been demonstrated with β-lactoglobulin, as its unique structure allows high solubility under harsh environmental conditions (Damodaran & Parkin, 2017). On the other hand, 100L-salt was significantly more soluble than 100L under neutral conditions. This finding can be related to the protein secondary structure observations, where 100L-salt had lower relative abundance of intermolecular β sheet and random coil than 100L (Fig. 4). Further, at certain concentrations and at specific pH, salt can uniquely affect electrostatic interactions and the bulk water structure around the protein, which likely enhanced hydration and increased protein solubility for 100L-salt (Hill et al., 1998; Meng & Ma, 2001; Von Hippel & Schleich, 1969).

While 100V was more soluble than 100L across all conditions, samples with higher 7S/11S ratio did not follow suit. Compounded environmental factors and differences in the protein structure, as influenced by fractionation conditions, contributed to differences in solubility more than differences in 7S/11S ratio did. Isolated environmental conditions need to be further explored to differentiate the impact of each factor from the 7S/11S ratio on protein solubility.

3.3.2. Gel strength

Like solubility, gelation properties are greatly impacted by the inherent protein profile. In soy protein, cysteine residues in 11S glycinin are especially important in forming inter- and intramolecular disulfide linkages, which are critical to establishing and strengthening the gel network (Hermansson, 1986; Nakamura, Utsumi, Kitamura, Harada, & Mori, 1984). However, for pea protein, hydrophobic interactions, hydrogen bonds, and electrostatic interactions have greater contribution to gel formation and strength than disulfide linkages (O'Kane, Happe, Vereijken, Gruppen, & Van Boekel, 2004b; Sun & Arntfield, 2010, 2012). The lower contribution of disulfide linkages to gel formation in pea protein compared to soy protein could be attributed to inherent differences in the structure and composition of 11S between species. Given these differences, it is unclear how 7S/11S ratio in pea could affect the reactions critical to gel formation. Therefore, in this study, the impact of 7S/11S ratios and salt on pea protein gel strength were evaluated.

cSPI formed a significantly stronger gel at 15% protein concentration than any of the pea protein samples at 20% protein concentration (Table 3), attributed to soy protein's inherent molecular properties. This observation was similar to previous reports comparing soy protein to pea protein gels (Hansen et al., 2022; O'Kane et al., 2004b; Shand, Ya, Pietrasik, & Wanasundara, 2007; Sun & Arntfield, 2012). Meanwhile, nPPI formed a significantly weaker gel structure than cPPI. cPPI was highly polymerized, and the formation of high molecular weight proteins may have enhanced its gel strength (Wang & Damodaran, 1990). Further, cPPI had lower protein purity than nPPI (79% versus 87%, respectively). Consequently, the gel strength of cPPI may have been enhanced by starch gelatinization (Kornet et al., 2021). Meanwhile, nPPI exhibited less polymerization and had significantly lower surface hydrophobicity (Table 2), which potentially reduced the protein-protein interactions necessary for gel network formation.

Among the isolated fractions and reconstituted isolates, gel strength increased with the abundance of vicilin (Table 3). 100V had low extent of polymerization (Fig. 1), was partially denatured (Table 2), and had high relative abundance of β sheet (Fig. 4), allowing it to form an organized gel network upon heating. Further, 100V's relatively low surface hydrophobicity and net surface charge might have achieved an ideal balance between attractive and repulsive forces, which contributed to the formation of a relatively strong gel network. In contrast, multiple factors inhibited strong gel formation for 100L. First, 100L was highly polymerized by disulfide linkages (Fig. 1) and intermolecular β sheet interactions (Fig. 4), which potentially caused the formation of insoluble aggregates, rather than a uniform gel network, upon heating. Large polymers also restrict strand flexibility during heating (O'Kane et al., 2005), which could have ultimately weakened the protein-protein interactions critical to gel formation for 100L. Secondly, the denaturation temperature of 100L was significantly higher than that of 100V (Table 2); therefore, 100L had greater resistance to unfolding than 100V during thermal treatment. Consequently, reactive sulfhydryl groups mostly likely remained buried within 100L's core and were thus inaccessible for gel formation. Additionally, the abundance of disulfide-linked polymers (Fig. 1) in 100L potentially reduced the availability of sulfhydryl groups needed for gel formation. Results also showed that with increasing abundance of 11S legumin in the reconstituted isolates and legumin-enriched nPPIs, there was a significant decrease in gel strength (Table 3). The discussed physicochemical properties of legumin also potentially interfered with the hydrophobic interactions, hydrogen bonding, and electrostatic interactions needed to form a strong gel.

Meanwhile, the effect of salt addition was significant for 100V but not for 100L. 100V-salt had a significantly higher gel strength than 100V (Table 3). The salt had a charge shielding effect, evidenced by the perceived higher surface hydrophobicity and lower surface charge (Table 2), which enhanced the noncovalent interactions among the 7S vicilin protein molecules and increased gel strength. On the other hand, the addition of salt in 100L enhanced the rigidity of the legumin proteins (Damodaran & Parkin, 2017), evidenced by the significantly higher denaturation temperature and enthalpy (Table 2). This stabilized protein structure in 100L-salt prevented the legumin proteins from unfolding, which is a necessary prerequisite for gel formation.

Considering the homology between pea and soy protein, the inferior gelling properties of the former has been frequently attributed to the lower abundance of 11S in pea compared to soy (Hansen et al., 2022). However, results of this work contradicted this assumption. Intrinsic differences between the two protein sources, in addition to the considerable variability in pea 11S legumin performance across different studies, must be alternatively considered. Similar to the results of this study, Barac et al. (2010), Bora et al. (1994), and Mession et al. (2015) reported that legumin formed weak gels. In contrast, O'Kane et al. (2004a, 2004b, 2005) produced strong gels from pea legumin fractions at protein concentrations as low as 10.5%. This controversy in the reported gelation properties of pea legumin is in stark contrast to the consistent gelling performance of soy 11S glycinin across different studies. The consistent gelling performance of soy 11S glycinin is attributed to years of breeding efforts to eliminate molecular variability (Mertens et al., 2012; Murphy & Resurreccion, 1984). In particular, the gelling performance of soy protein is attributed to soy glycinin consistently containing 8 cysteine residues per subunit, while pea legumin may contain anywhere from 2 to 7 (Casey & Short; 1981; Croy,

Gatehouse, Tyler, & Boulter, 1980; O'Kane et al., 2004b; Mession, Sok, Assifaoui, & Saurel, 2013). The relative lack of research on the inherent molecular properties of pea legumin, coupled with its wide compositional diversity both within and among cultivars, necessitate additional studies relating pea 11S legumin to gelation as well as other functional properties.

3.3.3. Emulsification capacity (EC)

cSPI had significantly higher EC than all pea protein samples (Table 3). Compared to the pea protein samples, cSPI had a favorable balance between surface hydrophobicity and surface charge (Table 2), which potentially allowed for efficient migration to the interface and the formation of protein films around the oil droplets. In contrast, cPPI had significantly lower surface charge and solubility than cSPI (Tables 2 and 3), which potentially caused a relatively unfavorable hydrophilic/lipophilic balance and significantly lower EC. Nevertheless, cPPI had a significantly higher EC than nPPI (Table 3). Compared to cPPI, nPPI was less denatured, had significantly lower surface hydrophobicity, and significantly higher solubility (Tables 2 and 3), which potentially disrupted nPPI's hydrophilic/lipophilic balance in favor of protein-water interactions.

Between the isolated fractions, 100V had a significantly higher EC than 100L (Table 3). This difference could be attributed to certain intrinsic characteristics of vicilin including its low molecular weight, which facilitates fast migration to the interface. Further, the high flexibility of vicilin due to lack of disulfide linkages allows it to easily orient at the interface (Liang & Tang, 2013). In contrast, legumin's high molecular weight and more compact structure may hinder migration to and orientation at the interface (Mession et al., 2015). Additionally, 100V was less polymerized (Fig. 1), had a high relative abundance of β sheet (Fig. 4), and had significantly higher solubility compared to 100L (Table 3), allowing it to have a relatively more balanced protein-water and protein-protein interactions at the interface.

Meanwhile, salt had a varied effect on the EC of the isolated fractions (Table 3). Addition of salt to 100L potentially increased the charge load on the protein, leading to enhanced protein-water interactions and improved hydrophilic/lipophilic balance, which consequently resulted in a significant increase in EC. Moreover, 100L-salt had a lower relative abundance of intermolecular β sheet and random coil than 100L (Fig. 4). This change in secondary structure may have contributed to the higher emulsification capacity in 100L-salt as compared to 100L, as proteins with ordered secondary structure have been reported as more efficient in stabilizing emulsions (Dagorn-Scaviner, Gueguen, & Lefebvre, 1987). However, other factors, such as the hydrophilic/lipophilic balance, molecular flexibility, and thickness of the interfacial film are also critical parameters in the emulsification behavior. This is demonstrated by the significantly lower EC of 100V-salt compared to 100V, despite its higher relative abundance of α helix. The charge shielding effect observed in 100V-salt (Table 2) negatively impacted the hydrophilic/lipophilic balance and likely overshadowed the potential influence of secondary structure on its emulsification capacity.

In comparison to 100V, increasing the proportion of 11S legumin negatively impacted EC, with significant reductions observed for 50V-50L, 20V-80L, and nPPI-80L. However, enriching nPPI with the low-performing fractionated legumin did not significantly cause further detriment to the EC. On the other hand, both nPPI-50L and nPPI-80L had significantly lower EC than 50V-50L and 20V-80L, respectively. These observations suggested that structural differences between legumin and vicilin imposed by fractionation, as well as the matrix effect, contributed more to the differences in EC than varying the 7S/11S ratio. The high polymerization and low solubility of the fractionated legumin, in comparison to fractionated vicilin, contributed the most to the observed differences in EC. Therefore, the impact of varying 7S/11S ratio on the emulsification behavior was not clearly distinguished.

3.4. Amino acid composition and PDCAAS of isolated fractions, reconstituted isolates, and legumin-enriched nPPIs

The amino acid composition of pea protein samples was evaluated to determine the proportion of key amino acids for structural and functional consideration. In general, all samples were rich in acidic amino acids but had a low percentage of sulfur-containing amino acids (Table 4). This finding agreed with previous reports of the amino acid composition of pea protein (Rutherfurd et al., 2014). Significant differences in the percent distribution of amino acids, except for that of hydrophobic amino acids, were noted among the samples.

cPPI had a significantly lower abundance of acidic and basic amino acids relative to the other samples, with the exception of 100V for acidic amino acids. This finding may be attributed to degradation of amino acids under the harsh extraction parameters typically used to produce cPPI. For example, lysine is especially sensitive to alkaline pH, higher extraction temperature, and longer extraction time (Feyzi, Varidi, Zare, & Varidi, 2018). Additionally, both aspartic and glutamic acid are deamidated under alkaline conditions coupled with adverse heat treatment (Damodaran & Parkin, 2017). Amino acid degradation can influence functional properties and nutritional quality of protein ingredients.

100L had a significantly higher content of sulfur-containing amino acids than 100V (Table 4). For the most part, samples with higher proportion of 11S legumin had a significantly higher percentage of sulfur-containing amino acids relative to nPPI and 100V. This observation was consistent with previous reports, though the amino acid composition of 11S legumin varied considerably within and across cultivars (Casey & Short, 1981; Choi, Taghvaei, Smith, & Ganjyal, 2022; Mession et al., 2013; Rangel, Domont, Pedrosa, & Ferreira, 2003). This reported

Table 4
Key amino acid (AA) percentage (g AA/100 g sample) and protein digestibility-corrected amino acid score (PDCAAS) of cPPI, nPPI, isolated fractions, reconstituted protein isolates, and legumin-enriched nPPIs with varying 7S vicilin to 11S legumin ratios.

Sample	Sulfur-containing AA (%)	Acidic AA (%)	Basic AA (%)	Ratio of Acidic to Basic AA	Hydrophobic AA (%)	Critical AA[a] (%)	PDCAAS[b]
cPPI	2.25 ± 0.03^{cdc}	28.3 ± 0.30^{c}	10.3 ± 0.26^{d}	2.74 ± 0.08^{a}	25.7 ± 3.25^{c}	13.4 ± 1.42^{b}	0.630 ± 0.01^{d*}
nPPI	1.81 ± 0.03^{ef}	35.2 ± 0.87^{a}	15.8 ± 0.49^{ab}	2.23 ± 0.01^{b}	27.9 ± 0.09	15.7 ± 0.25^{ab}	0.800 ± 0.01^{a}
100V	1.50 ± 0.05^{f}	28.8 ± 0.85^{c}	12.8 ± 0.37^{c}	2.24 ± 0.05^{b}	26.4 ± 1.04	17.2 ± 0.74^{ab}	0.389 ± 0.01^{e}
80V-20L	1.59 ± 0.04^{ef}	34.0 ± 0.81^{ab}	16.1 ± 0.33^{ab}	2.11 ± 0.01^{b}	29.9 ± 1.43	19.0 ± 1.54^{a}	0.594 ± 0.00^{d}
50V-50L	1.91 ± 0.04^{de}	33.0 ± 0.57^{ab}	16.3 ± 0.04^{a}	2.02 ± 0.03^{b}	30.6 ± 0.49	18.9 ± 0.34^{a}	0.649 ± 0.01^{cd}
nPPI-50LE	3.03 ± 0.06^{b}	30.6 ± 0.22^{bc}	14.5 ± 0.18^{bc}	2.12 ± 0.04^{b}	27.1 ± 0.48	14.8 ± 0.30^{ab}	0.632 ± 0.01^{d}
20V-80L	2.49 ± 0.07^{c}	33.2 ± 1.01^{ab}	16.1 ± 0.56^{ab}	2.07 ± 0.06^{b}	29.8 ± 0.14	17.8 ± 0.44^{a}	0.654 ± 0.01^{bcd}
nPPI-80LE	3.02 ± 0.13^{b}	35.1 ± 0.65^{a}	17.0 ± 0.35^{a}	2.07 ± 0.06^{b}	30.4 ± 0.99	16.9 ± 0.74^{ab}	0.736 ± 0.02^{abc}
100L	3.87 ± 0.08^{a}	36.2 ± 0.20^{a}	17.4 ± 0.19^{a}	2.08 ± 0.03^{b}	29.6 ± 0.26	16.5 ± 0.25^{ab}	0.742 ± 0.00^{ab}

[a] Calculated as the % sum of valine, isoleucine, leucine, and phenylalanine.

[b] Calculated based on the recommended amino acid scoring pattern for children (2–5 years) (FAO/WHO Expert Consultation, 1991) and an *in vitro* digestibility of ≥100% measured for all pea protein samples.

[c] Lowercase letters indicate significant differences among the means (n = 3; n = 2 for PDCAAS) in each column, according to the Tukey-Kramer multiple means comparison test ($P < 0.05$); [c]No significant differences in hydrophobic amino acids were detected among pea protein samples, according to the Tukey-Kramer multiple means comparison test ($P < 0.05$).

variation could explain the lack of significant difference in the amount of sulfur-containing amino acids between cPPI and 50V-50L or 20V-80L, despite their high abundance of 11S legumin. However, the high relative abundance of sulfur-containing amino acids did not correspond to enhanced gelling properties (Tables 3 and 4). This observation might indicate that the cysteine residues in 11S legumin in pea have little contribution to gel strength, in stark contrast to soy 11S glycinin, as discussed. However, the noted polymerization of the isolated 11S legumin (Fig. 1, lane 10), could have contributed to a comparatively low gel strength.

Significant differences between 100L and 100V were also noted in their percentage of acidic amino acids and basic amino acids (Table 4). 100L contained significantly more acidic and basic amino acids than 100V. The latter finding agreed with Barac et al. (2010), who reported 7S vicilin contained less basic amino acids than 11S legumin. Since 100V was lower in both acidic and basic amino acids compared to 100L, the ratio was not significantly different from the other samples. The relative ratio of acidic and basic amino acids determines the net charge on the surface of protein (Tang, Chen, & Ma, 2009). This observation is consistent with the lack of significant difference in zeta potential at pH 7 (Table 2).

On the other hand, 100V contained significantly more critical amino acids than 100L. There were a few minor statistical differences in the abundance of critical amino acids among the remaining pea protein samples. However, as the percentage of critical amino acids for all pea protein samples were below the theoretical critical value of 28%, this difference likely imparted negligible practical impact on functionality among the samples (Mo, Zhong, Wang, & Sun, 2006). Of the hydrophobic amino acids, phenylalanine, leucine, isoleucine, and valine are critical because of their degree of hydrophobicity compared to other hydrophobic residues (Mo et al., 2006). If these amino acids comprise more than 28% of the total amino acids, hydrophobic interactions will offset any electrostatic interactions, resulting in protein aggregation and minimal solubility across a wide pH range. The percentages of these critical amino acids in all samples were similar to what is reported for the acidic subunit (20.1%) of soy 11S glycinin (Mo et al., 2006). This observation could partially explain the good overall solubility of nPPI, 100V, 100L, reconstituted and legumin enriched nPPI samples at both pH 7 and 3.4 (Table 3).

In terms of nutritional quality, all pea protein samples had high *in vitro* digestibility (≥100%, results not shown). Thus, their PDCAAS was equal to the amino acid score (AAS) (Table 4). The PDCAAS of 100L was significantly higher than that of 100V. Consequently, increasing the abundance of 11S legumin significantly raised the PDCAAS of reconstituted isolates compared to 100V. On the other hand, legumin enrichment did not improve the PDCAAS of either nPPI-50LE or nPPI-80LE (Table 4). While nPPI was limited by cysteine and methionine, similar to what was reported by Rutherfurd et al. (2014), cPPI, 100L, legumin-enriched nPPIs, 20V-80L, and 50V-50L were limited by threonine (data not shown). Cysteine, methionine, and threonine are among the most susceptible amino acids to alkaline pH, long extraction time, and higher extraction and drying temperatures (Damodaran & Parkin, 2017; De Groot & Slump, 1969; Feyzi et al., 2018). Thus, relative to nPPI, harsher extraction parameters for the isolated fractions and cPPI may have degraded susceptible amino acid residues, resulting in reduced PDCAAS. Meanwhile, while threonine and sulfur-containing amino acids were also low in 100V and 80V-20L, tryptophan was the limiting amino acid in these samples. This observation was consistent with previous reports of vicilin containing significantly less tryptophan than legumin (Danielsson, 1949; Derbyshire et al., 1976; Rangel et al., 2003). Ultimately, the observed variation in PDCAAS among cPPI, nPPI, and the reconstituted and enriched samples may be in part due to the protein extraction conditions.

4. Conclusions

This study is the first to thoroughly characterize the impact of 7S/11S ratio on pea protein structure, functionality, and nutritional quality. Apart from combining fractionated 7S vicilin and 11S legumin in different ratios, for the first time pea protein isolate was enriched with 11S legumin to test the impact of higher abundance of 11S legumin on functionality and nutritional quality within an unfractionated protein matrix. The work shed doubt on the common assumption that the differences in 11S abundance between pea and soy is the main reason behind pea protein's inferior functionality. In fact, results showed that the isolated vicilin fraction had greater solubility, gel strength, and emulsification capacity than the isolated legumin fraction. Further, legumin enrichment within the matrix of pea protein isolate did not improve protein functionality or nutritional quality. These observations were in stark contrast to what has been documented for soy protein, which credits higher abundance of 11S glycinin and its sulfur-containing amino acids as the factors behind greater functionality and nutritional quality. While the findings of this study indicated that pea 7S vicilin has greater functionality but lower nutritional quality than pea 11S legumin, further investigation is warranted to determine the isolated impact of genetic variance and molecular heterogeneity on protein functionality and nutritional quality. Although fractionation was successful in producing vicilin and legumin rich fractions, the process resulted in structural changes (especially for the legumin rich fraction) that could have contributed to the observed functionality and nutritional quality, potentially convoluting the effect of the 7S vicilin to 11S legumin ratio. Nevertheless, this work provided foundational knowledge that will provide guidance for future studies aiming at predicting pea protein functionality and nutritional quality to subsequently devise strategies to improve the quality and consistency of pea protein ingredients.

Funding

This work was generously supported by the Plant Protein Innovation Center.

CRediT author statement

Holly Husband- Conceptualization, Methodology, Investigation, Formal analysis, Visualization, Writing – original draft, review, & editing. Sungil Ferreira- Methodology, Investigation, Writing – review. Fan Bu- Formal analysis, Visualization, Writing – review. Samira Feyzi- Methodology, Writing – review. Baraem P. Ismail- Conceptualization, Supervision, Project administration, Writing – review & editing, Funding acquisition

Declaration of competing interest

None.

Data availability

The data that has been used is confidential.

Acknowledgements

The authors would like to acknowledge Christopher Sherve for his help with molecular weight distribution analysis by size exclusion chromatography. FTIR-ATR data collection was done in the Characterization Facility, University of Minnesota, which receives partial support from the NSF through the MRSEC (Award Number DMR-2011401) and the NNCI (Award Number ECCS-2025124) programs.

Appendix A. Supplementary data

Supplementary data to this article can be found online at https://doi.org/10.1016/j.foodhyd.2023.109429.

References

Barac, M., Cabrilo, S., Pesic, M., Stanojevic, S., Zilic, S., Macej, O., et al. (2010). Profile and functional properties of seed proteins from six pea (Pisum sativum) genotypes. *International Journal of Molecular Sciences, 11*(12), 4973–4990.

Barac, M. B., Pesic, M. B., Stanojevic, S. P., Kostic, A. Z., & Cabrilo, S. B. (2015). Technofunctional properties of pea (Pisum sativum) protein isolates: A review. *Acta Periodica Technologica*, (46), 1–18.

Bora, P., Brekke, C., & Powers, J. (1994). Heat induced gelation of pea (Pisum sativum) mixed globulins, vicilin and legumin. *Journal of Food Science, 59*(3), 594–596.

Boyle, C., Hansen, L., Hinnenkamp, C., & Ismail, B. (2018). Emerging camelina protein: Extraction, modification, and structural/functional characterization. *Journal of the American Oil Chemists' Society, 95*(8), 1049–1062.

Bruckner-Guhmann, M., Heiden-Hecht, T., Sozer, N., & Drusch, S. (2018). Foaming characteristics of oat protein and modification by partial hydrolysis. *European Food Research and Technology, 244*(12), 2095–2106.

Bu, F., Feyzi, S., Nayak, G., Mao, Q., Kondeti, V., Bruggeman, P., … Ismail, B. (2023). Investigation of novel cold atmospheric plasma sources and their impact on the structural and functional characteristics of pea protein. *Innovative Food Science & Emerging Technologies: IFSET: The Official Scientific Journal of the European Federation of Food Science and Technology, 83*, Article 103248.

Bu, F., Nayak, G., Bruggeman, P., Annor, G., & Ismail, B. (2022). Impact of plasma reactive species on the structure and functionality of pea protein isolate. *Food Chemistry, 371*, Article 131135.

Cao, & Mezzenga, R. (2019). Food protein amyloid fibrils: Origin, structure, formation, characterization, applications, and health implications. *Advances in Colloid and Interface Science, 269*, 334–356. https://doi.org/10.1016/j.cis.2019.05.002

Casey, R., & Domoney, C. (1999). Pea globulins. In *Seed proteins* (pp. 171–208). Dordrecht: Springer Netherlands.

Casey, R., Sharman, J., Wright, D., Bacon, J., & Guldager, P. (1982). Quantitative variability in Pisum seed globulins: Its assessment and significance. Qualitas Plantarum. *Plant Foods for Human Nutrition, 31*(4), 333–346.

Casey, R., & Short, M. (1981). Variation in amino acid composition of legumin from Pisum. *Phytochemistry, 20*(1), 21–23.

Choi, H., Taghvaei, M., Smith, B., & Ganjyal, G. (2022). Biochemical analysis of protein compositions among pea (Pisum sativum) cultivars grown in the Northwest USA. *ACS Food Science & Technology, 2*(7), 1067–1076.

Clark, A. H., Kavanagh, G. M., & Ross-Murphy, S. B. (2001). Globular protein gelation—theory and experiment. *Food Hydrocolloids, 15*(4–6), 383–400.

Croy, R., Gatehouse, J., Tyler, M., & Boulter, D. (1980). The purification and characterization of a third storage protein (convicilin) from the seeds of pea (Pisum sativum L.). *Biochemical Journal, 191*(2), 509–516.

Dagorn-Scaviner, C., Gueguen, J., & Lefebvre, J. (1986). Comparison of interfacial behaviours of pea (Pisum sativum L.) legumin and vicilin at air/water interface. *Die Nahrung, 30*(3/4), 337–347.

Dagorn-Scaviner, C., Gueguen, J., & Lefebvre, J. (1987). Emulsifying properties of pea globulins as related to their adsorption behaviors. *Journal of Food Science, 52*(2), 335–341.

Damodaran, S. (1988). Refolding of thermally unfolded soy proteins during the cooling regime of the gelation process: Effect on gelation. *Journal of Agricultural and Food Chemistry, 36*(2), 262–269.

Damodaran, S., & Parkin, K. (2017). *Fennema's food chemistry* (5th ed.). Boca Raton: CRC Press.

Danielsson, C. (1949). Seed globulins of the gramineae and leguminosae. *Biochemical Journal, 44*(4), 387–400.

De Groot, A., & Slump, P. (1969). Effects of severe alkali treatment of proteins on amino acid composition and nutritive value. *The Journal of Nutrition, 98*(1), 45–56.

Derbyshire, E., Wright, D., & Boulter, D. (1976). Legumin and vicilin, storage proteins of legume seeds. *Phytochemistry, 15*(1), 3–24.

FAO/WHO Expert Consultation. (1991). *Protein quality evaluation*.

Feyzi, S., Varidi, M., Zare, F., & Varidi, M. (2018). Effect of drying methods on the structure, thermo and functional properties of fenugreek (Trigonella foenum graecum) protein isolate. *Journal of the Science of Food and Agriculture, 98*(5), 1880–1888.

Foegeding, E., & Davis, J. (2011). Food protein functionality: A comprehensive approach. *Food Hydrocolloids, 25*(8), 1853–1864.

Gatehouse, J., Lycett, G., Croy, R., & Boulter, D. (1982). The post-translational proteolysis of the subunits of vicilin from pea (Pisum sativum L.). *Biochemical Journal, 207*(3), 629–632.

Grossmann, L., & McClements, D. J. (2022). *Current insights into protein solubility: A review of its importance for alternative proteins*. Food Hydrocolloids, Article 108416.

Gueguen, J., & Barbot, J. (1988). Quantitative and qualitative variability of pea (Pisum sativum L.) protein composition. *Journal of the Science of Food and Agriculture, 42*(3), 209–224.

Gueguen, J., Vu, A., & Schaeffer, F. (1984). Large-scale purification and characterisation of pea globulins. *Journal of the Science of Food and Agriculture, 35*(9), 1024–1033.

Guo, M. Q., Hu, X., Wang, C., & Ai, L. (2017). Polysaccharides: Structure and solubility. *Solubility of Polysaccharides*. https://doi.org/10.5772/intechopen.71570

Hansen, L., Bu, F., & Ismail, B. (2022). Structure-function guided extraction and scale-up of pea protein isolate production. *Foods, 11*(23), 3773.

Hermansson, A. (1986). Soy protein gelation. *Journal of the American Oil Chemists' Society, 63*(5), 658–666.

Hill, S. E., Ledward, D. A., & Mitchell, J. R. (1998). Functional properties of food macromolecules. In S. E. Hill, D. A. Ledward, & J. R. Mitchell (Eds.), *Chapman & Hall food science book* (2nd ed.). Gaithersburg, Md: Aspen.

Hinnenkamp, C., & Ismail, B. (2021). Enhancing emulsion stability: The synergistic effect of combining Procream and partially hydrolyzed whey protein. *International Dairy Journal, 119*, Article 105059.

Housmans, J. A., Houben, B., Monge-Morera, M., Asvestas, D., Nguyen, H. H., Tsaka, G., … Schymkowitz, J. (2022). Investigating the sequence determinants of the curling of amyloid fibrils using ovalbumin as a case study. *Biomacromolecules, 23*(9), 3779–3797.

Kimura, A., Fukuda, T., Zhang, M., Motoyama, S., Maruyama, N., & Utsumi, S. (2008). Comparison of physicochemical properties of 7S and 11S globulins from pea, Fava bean, cowpea, and French bean with those of soybean, French bean 7S globulin exhibits excellent properties. *Journal of Agricultural and Food Chemistry, 56*(21), 10273–10279.

Kornet, R., Veenemans, J., Venema, P., Van der Goot, A., Meinders, M., Sagis, L., et al. (2021). Less is more: Limited fractionation yields stronger gels for pea proteins. *Food Hydrocolloids, 112*, Article 106285.

Koyoro, H., & Powers, J. (1987). Functional properties of pea globulin fractions. *Cereal Chemistry, 64*(2), 97–101.

La Cour, R., Jorgensen, H., & Schjoerring, J. (2019). Improvement of tryptophan analysis by liquid chromatography-single quadrupole Mass spectrometry through the evaluation of multiple parameters. *Frontiers in Chemistry, 7*, 797.

Lam, A., Warkentin, T., Tyler, R., & Nickerson, M. (2017). Physicochemical and functional properties of protein isolates obtained from several pea cultivars. *Cereal Chemistry, 94*(1), 89–97.

Liang, H., & Tang, C. (2013). Emulsifying and interfacial properties of vicilins: Role of conformational flexibility at quaternary and/or tertiary levels. *Journal of Agricultural and Food Chemistry, 61*(46), 11140–11150.

Marti, Bock, J. E., Pagani, M. A., Ismail, B., & Seetharaman, K. (2016). Structural characterization of proteins in wheat flour doughs enriched with intermediate wheatgrass (Thinopyrum intermedium) flour. *Food Chemistry, 194*, 994–1002. https://doi.org/10.1016/j.foodchem.2015.08.082

Maruyama, N., Salleh, M., Takahashi, K., Yagasaki, K., Goto, H., Hontani, N., … Utsumi, S. (2002). The effect of the N-linked glycans on structural features and physicochemical functions of soybean β-conglycinin homotrimers. *Journal of the American Oil Chemists' Society, 79*(2), 139–144.

Matta, N., Gatehouse, J., & Boulter, D. (1981). Molecular and subunit heterogeneity of legumin of pisum sativum L. (Garden pea)— a Multi-dimensional gel electrophoretic study. *Journal of Experimental Botany, 32*(6), 1295–1307.

McClements, D., & Grossmann, L. (2022). *Next-generation plant-based foods: Design, production, and properties*. Cham, Switzerland: Springer.

Meng, G., & Ma, C. (2001). Thermal properties of Phaseolus angularis (red bean) globulin. *Food Chemistry, 73*(4), 453–460.

Mertens, C., Dehon, L., Bourgeois, A., Verhaeghe-Cartrysse, C., & Blecker, C. (2012). Agronomical factors influencing the legumin/vicilin ratio in pea (Pisum sativum L.) seeds. *Journal of the Science of Food and Agriculture, 92*(8), 1591–1596.

Mession, J., Assifaoui, A., Cayot, P., & Saurel, R. (2012). Effect of pea proteins extraction and vicilin/legumin fractionation on the phase behavior in admixture with alginate. *Food Hydrocolloids, 29*(2), 335–346.

Mession, J., Chihi, M., Sok, N., & Saurel, R. (2015). Effect of globular pea proteins fractionation on their heat-induced aggregation and acid cold-set gelation. *Food Hydrocolloids, 46*, 233–243.

Mession, J., Sok, N., Assifaoui, A., & Saurel, R. (2013). Thermal denaturation of pea globulins (Pisum sativum L.) molecular interactions leading to heat-induced protein aggregation. *Journal of Agricultural and Food Chemistry, 61*(6), 1196–1204.

Mo, X., Zhong, Z., Wang, D., & Sun, X. (2006). Soybean glycinin subunits: Characterization of physicochemical and adhesion properties. *Journal of Agricultural and Food Chemistry, 54*(20), 7589–7593.

Murphy, P., & Resurreccion, A. (1984). Varietal and environmental differences in soybean glycinin and beta.-conglycinin content. *Journal of Agricultural and Food Chemistry, 32*(4), 911–915.

Mwasaru, M., Muhammad, K., Bakar, J., & Che Man, Y. (1999). Effects of isolation technique and conditions on the extractability, physicochemical and functional properties of pigeonpea (Cajanus cajan) and cowpea (Vigna unguiculata) protein isolates. II. Functional properties. *Food Chemistry, 67*(4), 445–452.

Nakamura, T., Utsumi, S., Kitamura, K., Harada, K., & Mori, T. (1984). Cultivar differences in gelling characteristics of soybean glycinin. *Journal of Agricultural and Food Chemistry, 32*(3), 647–651.

Nosworthy, M. G., & House, J. D. (2017). Factors influencing the quality of dietary proteins: Implications for pulses. *Cereal Chemistry, 94*(1), 49–57. https://doi.org/10.1094/CCHEM-04-16-0104-FI

O'Kane, F., Happe, R., Vereijken, J., Gruppen, H., & Van Boekel, M. (2004a). Characterization of pea vicilin. 2. Consequences of compositional heterogeneity on heat-induced gelation behavior. *Journal of Agricultural and Food Chemistry, 52*(10), 3149–3154.

O'Kane, F., Happe, R., Vereijken, J., Gruppen, H., & Van Boekel, M. (2004b). Heat-induced gelation of pea legumin: Comparison with soybean glycinin. *Journal of Agricultural and Food Chemistry, 52*(16), 5071–5078.

O'Kane, Vereijken, J. M., Gruppen, H., & Van Boekel, M. A. J. S. (2005). Gelation behavior of protein isolates extracted from 5 cultivars of Pisum sativum L. *Journal of*

Food Science, 70(2), C132–C137. https://doi.org/10.1111/j.1365-2621.2005.tb07073.x

Pedrosa, C., Trisciuzzi, C., & Ferreira, S. (1997). Effects of glycosylation on functional properties of vicilin, the 7S storage globulin from pea (Pisum sativum). *Journal of Agricultural and Food Chemistry, 45*(6), 2025–2030.

Rangel, A., Domont, G., Pedrosa, C., & Ferreira, S. (2003). Functional properties of purified vicilins from cowpea (Vigna unguiculata) and pea (Pisum sativum) and cowpea protein isolate. *Journal of Agricultural and Food Chemistry, 51*(19), 5792–5797.

Rickert, D., Johnson, L., & Murphy, P. (2004). Functional properties of improved glycinin and β conglycinin fractions. *Journal of Food Science, 69*(4), FCT303–FCT311.

Rutherfurd, S. M., Fanning, A. C., Miller, B. J., & Moughan, P. J. (2014). Protein digestibility-corrected amino acid scores and digestible indispensable amino acid scores differentially describe protein quality in growing Male rats. *The Journal of Nutrition Methodology and Mathematical Modeling*. https://doi.org/10.3945/jn.114.195438

Sadat, A., & Joye, I. J. (2020). Peak fitting applied to fourier transform infrared and Raman spectroscopic analysis of proteins. *Applied Sciences, 10*(17), 5918.

Schroeder, H. (1982). Quantitative studies on the cotyledonary proteins in the genus Pisum. *Journal of the Science of Food and Agriculture, 33*(7), 623–633.

Shand, P., Ya, H., Pietrasik, Z., & Wanasundara, P. (2007). Physicochemical and textural properties of heat-induced pea protein isolate gels. *Food Chemistry, 102*(4), 1119–1130.

Suchkov, V., Popello, I., Grinberg, V., & Tolstoguzov, V. (1990). Isolation and purification of 7S and 11S globulins from broad beans and peas. *Journal of Agricultural and Food Chemistry, 38*(1), 92–95.

Sun, X., & Arntfield, S. (2010). Gelation properties of salt-extracted pea protein induced by heat treatment. *Food Research International, 43*(2), 509–515.

Sun, X., & Arntfield, S. (2012). Molecular forces involved in heat-induced pea protein gelation: Effects of various reagents on the rheological properties of salt-extracted pea protein gels. *Food Hydrocolloids, 28*(2), 325–332.

Tang, C., Chen, L., & Ma, C. (2009). Thermal aggregation, amino acid composition and in vitro digestibility of vicilin-rich protein isolates from three phaseolus legumes: A comparative study. *Food Chemistry, 113*(4), 957–963.

Tang, C., Choi, S., & Ma, C. (2007). Study of thermal properties and heat-induced denaturation and aggregation of soy proteins by modulated differential scanning calorimetry. *International Journal of Biological Macromolecules, 40*(2), 96–104.

Temtrirath, K. (2022). A UHPLC-PDA method for the quantitative analysis of total amino acids in infant formula with microwave-assisted acid hydrolysis. *Chemical Papers, 76*(5), 3065–3076.

Tulbek, M. C., Lam, R. S. H., Wang, Y. C., Asavajaru, P., & Lam, A. (2017). Pea: A sustainable vegetable protein crop. In *Sustainable protein sources* (pp. 145–164). https://doi.org/10.1016/B978-0-12-802778-3.00009-3

Tzitzikas, E., Vincken, J., De Groot, J., Gruppen, H., & Visser, R. (2006). Genetic variation in pea seed globulin composition. *Journal of Agricultural and Food Chemistry, 54*(2), 425–433.

Uzzan, A. L. D. O. (1988). Vegetable protein products from seeds: Technology and uses in the food industry. *Developments in Food Proteins*.

Von Hippel, P., & Schleich, T. (1969). Ion effects on the solution structure of biological macromolecules. *Accounts of Chemical Research, 2*(9), 257–265.

Waggle, D. H., Steinke, F. H., & Shen, J. L. (1989). *Isolated soy proteins*.

Wang, & Damodaran, S. (1990). Thermal gelation of globular proteins: Weight-average molecular weight dependence of gel strength. *Journal of Agricultural and Food Chemistry, 38*(5), 1157–1164. https://doi.org/10.1021/jf00095a001

Wang, Q., & Ismail, B. (2012). Effect of Maillard-induced glycosylation on the nutritional quality, solubility, thermal stability and molecular configuration of whey protein. *International Dairy Journal, 25*(2), 112–122.

Zhao, H., Shen, C., Wu, Z., Zhang, Z., & Xu, C. (2020). Comparison of wheat, soybean, rice, and pea protein properties for effective applications in food products. *Journal of Food Biochemistry, 44*(4), Article E13157.

Web References

Grand View Research. (2021). *Pea protein market size, share & trends analysis report by* product (Hydrolysate, isolates, concentrates, Textured), by application (Meat substitutes, dietary supplement, Bakery goods), by region, and segment Forecasts, *2021 – 2028*. Retrieved from: https://www.grandviewresearch.com/industry-analysis/pea-protein-market Accessed December 7, 2022.

SPINS/GFI. (2021). U.S. retail market data for the plant-based industry. Retrieved from https://gfi.org/marketresearch/ Accessed November 21, 2022.